UNIVERSIDADE DE LISBOA
FACULDADE DE CIÊNCIAS
DEPARTAMENTO ENGENHARIA GEOGRÁFICA, GEOFÍSICA E ENERGIA

Vegetation Carbon Losses Linked to Mediterranean Extreme Events

Tiago Miguel Rivero Ermitão Rodrigues da Silva

Mestrado em Ciências Geofísicas
Especialização em Meteorologia e Oceanografia

Dissertação orientada por:
Doutora Ana Cristina Machado Russo
Doutora Célia Marina Pedroso Gouveia

2021

Acknowledgements

First of all, I would like to thank to my thesis supervisors, Ana Russo and professora Célia Gouveia. Thanks for all the help and availability, for have believed in my work and capacities, for the commitment and effort made to successfully help me finish this work, for all the hints and advice they gave me to make me surpass all the difficulties and, most importantly, for contributing to continue to make me believe that meteorology and climatology, and the contribute to the advance of science, are essential, and this is the career I want to pursue in the future.

Also, I would like to thank to my friends, an important part in my life, especially the ones from the university, for all the friendship and generosity, all the difficulties, but also the great moments and memories we have shared together during these last six years. A very important thanks to my friend, and work colleague, Joana, for all the support she gave me, all the friendship and all the patience during all these years, and all the hints and advice given in this work that helped me to accomplish this goal, which without them, this path would be harder to achieve.

Thanks to my colleagues in laboratory 8.3.15 that received me well since the first weeks, and especially to Silvia that was always available to help me and to give me hints to overcome the problems and to Patricia to help me in the early stages to manage and process the initial data of this work.

A very, very special thanks to my parents, for being so supportive, generous, and comprehensive, and closely accompanied me, in my academic path and my life, and because without them, this path would be completely impossible.

Finally, this work was supported by FCT through projects IMPECAF (PTDC/CTA-CLI/28902/2017).

Resumo

A atividade dos ecossistemas terrestres é particularmente suscetível à variabilidade climática e, face às mudanças globais e regionais que têm vindo a ocorrer, tem reagido com rápidas mudanças no ciclo de vegetação natural, na produtividade das plantas e na absorção de carbono terrestre. Os eventos climáticos extremos, nomeadamente as secas, as ondas de calor e os grandes fogos associados, têm sido reconhecidos por terem um papel preponderante na alteração da dinâmica dos ecossistemas. A ocorrência de condições quentes e secas alteram a dinâmica da vegetação e perturbam severamente os regimes fotossintéticos, levando a fortes perdas de produtividade das plantas e, consequentemente, a fortes anomalias na regulação do mecanismo de absorção de carbono dos ecossistemas. Além disso, o aumento da frequência e severidade destes eventos climáticos extremos, como reportado nos recentes relatórios do IPCC, contribuirá para a intensificação das perturbações nos sistemas terrestres que absorvem carbono, desestabilizando o ciclo de carbono e contribuindo, consequentemente, para o aumento de CO_2 na atmosfera.

Os eventos de seca são reconhecidos, entre uma ampla gama de eventos extremos, por desempenharem um papel crucial no ciclo de carbono devido às perturbações que induzem na fotossíntese e na absorção de carbono. Por sua vez, o aumento da frequência e severidade das secas terá impactos a curto-médio prazo, mas também, a longo prazo, devido aos efeitos continuados que têm nos ecossistemas, inibindo-os de recuperar e regenerar. Dessa forma, ao longo de vários meses, a produtividade das plantas estará perturbada, podendo ter consequências desastrosas e permanentes na dinâmica vegetação. Além disso, estes eventos têm o potencial de aumentar o risco de incêndios devido à maior vulnerabilidade dos ecossistemas, elevando as perdas de produtividade das plantas, e contribuindo, geralmente, para atrasar o seu processo de regeneração durante muito tempo.

A Europa, e em particular, a região do Mediterrâneo, têm sido afetadas por secas severas e grandes fogos nas últimas décadas, sendo uma região particularmente sensível a fenómenos extremos. Nos últimos anos, vários estudos têm comprovado e analisado os impactos que estes eventos têm na vegetação e o seu contributo para a diminuição do carbono armazenado nos ecossistemas da região. No entanto, vários desses estudos observaram que o acoplamento clima-vegetação, ou seja, a relação que existe entre a influência do evento climático e a resposta da vegetação não é fácil de estabelecer, tendo em conta que o efeito extremo do evento climático nem sempre gera uma resposta extrema a nível ecológico.

Tendo em conta as premissas anteriores, estre trabalho propõe-se a avaliar o impacto de um conjunto de secas severas e grandes fogos, ocorridos entre 2001 e 2019, em três regiões diferentes da bacia do Mediterrâneo (Península Ibérica, Itália e Grécia, e França), pretendendo analisar a sua influência na vegetação. Será avaliada a persistência de condições secas no solo e o número de meses em que a sua normal atividade é perturbada, bem como a perturbação de cada evento extremo no balanço anual de produtividade da vegetação de cada região. Foram utilizados produtos de deteção remota para monitorizar a produtividade dos ecossistemas, nomeadamente o Gross Primary Production (GPP) e o Net Photosynthesis (PsNet), para analisar a quantidade de água no solo foi utilizado o produto ESA CCI Soil Moisture (SM) e para detetar áreas queimadas foi utilizada a área ardida do produto FIRECCI. A qualidade de todos estes produtos de deteção remota foi analisada, de modo a conhecer a sua precisão para a monitorização e a sua capacidade de capturar os efeitos dos eventos climáticos extremos nos ecossistemas na região do Mediterrâneo.

A análise da quantidade de água no solo e produção primária da vegetação, para o período mencionado, permitiram identificar os eventos de seca mais severos e que tiveram maiores impactos nos ecossistemas. Recorrendo a métricas estatísticas, como a determinação, ao longo do período de análise 2001-2019, do desvio padrão médio mensal da produtividade da vegetação, foi possível a identificação

das áreas mais afetadas por condições de seca prolongadas. Além disso, com base no cálculo do percentil 25 das anomalias de SM, de forma a identificar os períodos com maiores deficits de disponibilidade de água no solo, foi possível reconhecer as regiões cujos ecossistemas foram fortemente perturbados por eventos extremos.

Na Península Ibérica, os episódios de 2005 e 2012 provocaram amplas alterações na atividade da vegetação. Na generalidade, em ambos os casos de estudo, as regiões mais afetadas foram o oeste e o sul da Península Ibérica. Várias áreas revelaram uma elevada falta de água no solo na primavera, que conduziu a impactos severos no estado e na atividade das plantas durante muitos meses. A severidade do evento de 2005, que levou a perdas de produtividade líquida de ~ 40 TgC/ano, conjugada com condições climáticas pouco propícias ao processo de recuperação nos meses seguintes, levaram a um prolongamento das anomalias da produtividade na vegetação afetada. Dessa forma, houve um aumento das perdas de fotossíntese líquida durante um intervalo de tempo longo, o que afetou profundamente a dinâmica da vegetação.

Na região da Itália e Grécia, os eventos de 2003, 2007 e 2012 afetaram os ecossistemas de cerca de 30-35% do território, destacando-se especialmente o ano de 2007 pela sua intensidade, devido ao efeito combinado de um evento de seca, intensas ondas de calor no verão e grandes fogos. Dada a sua grande complexidade, este evento composto levou a uma forte inibição da recuperação da vegetação afetada nos meses seguintes, amplificando as perdas anuais de produtividade até ~ 24 TgC no período entre 2007 e 2009. Apesar de menos intensos, os eventos de seca de 2003 e 2012 geraram fortes deficits de água no solo, promovendo fortes anomalias na dinâmica das plantas, principalmente nos meses de verão.

Em França, o episódio de 2006 afetou mais de 25% da vegetação do território devido às condições de seca severas que perturbaram a produção dos ecossistemas durante 3 a 5 meses em diversas áreas, e induziu perdas anuais de produtividade de ~ 25 TgC/ano.

A ocorrência de épocas de fogo severas está intimamente associada à disponibilidade de biomassa de combustão rápida na presença de um evento climático extremo. A conjugação desses fatores despoletou épocas de fogos catastróficas, nomeadamente em 2003 e 2017 na Península Ibérica e 2007 na Itália e Grécia, associadas a intensas ondas de calor no verão, e 2005 e 2012 na Península Ibérica e 2012 na Itália e Grécia, associadas a condições de seca muito persistentes. Em todos os casos de estudo, a vegetação demorou vários meses a conseguir recuperar a atividade fotossintética normal, mesmo quando as condições climáticas foram favoráveis, demonstrando o impacto que as épocas de fogo severas têm na dinâmica dos ecossistemas.

A avaliação das perturbações na atividade fotossintética causadas por secas e grandes incêndios permitiram quantificar as perdas de produtividade da vegetação e, ainda, a avaliação do seu processo de recuperação nos meses seguintes. A resposta dos ecossistemas varia amplamente, podendo demorar meses a anos a recuperar a atividade fotossintética normal. Essa resposta depende das condições climáticas nos meses seguintes e do tipo de cobertura vegetal afetada. As perturbações induzidas na atividade da vegetação, provocadas por eventos de seca são significativamente maiores do que as provocadas por incêndios, especialmente devido à sua maior área afetada. Além disso, as secas possuem uma escala temporal muito maior, o que induz mais perturbações na produtividade das plantas durante um longo intervalo de tempo. No entanto, apesar de os fogos corresponderem a eventos de menor duração, podem inibir fortemente a vegetação de regenerar, amplificando as perdas nos ecossistemas durante vários meses.

Palavras-Chave: Secas, Grandes Incêndios, Recuperação da Vegetação, Perdas de Produtividade

Abstract

The activity of terrestrial ecosystems is particularly susceptible to the climate variability and, facing the recently global and regional changes, has been responding with rapid changes on natural vegetation cycle, plants productivity and terrestrial carbon uptake.

Droughts have been broadly recognized, among a wide range of extreme events, as playing a central role on the carbon cycle. Dry permanent conditions contribute to the occurrence of high hydric stress on vegetation, generating disturbances on the regular photosynthesis, carbon uptake and regular plants mechanisms. Furthermore, they may increase the risk of fires due to the higher vulnerability of ecosystems, enhancing the losses on vegetation productivity, and inhibiting, generally, their regeneration process for a long time.

Europe, and in particular, the Mediterranean region, has been affected by severe droughts and large fires in the last decades, being an area particularly sensitive to extreme phenomena. Therefore, this work proposes to assess the impact of a set of the severest droughts and large fires, between 2001 and 2019, over three different regions of Mediterranean basin (Iberian Peninsula, Italy and Greece, and France), attempting to analyse their influence on vegetation. It will be assessed the persistence of soil dry conditions and the number of months that the normal activity of vegetation is disturbed. Remote sense products were used to monitor the plant's productivity, to assess the soil moisture and to detect burned areas.

The analysis of soil moisture and primary production of vegetation, for the referred study period, allowed to identify the most hazardous drought events which had larger impacts on ecosystems. Over Iberian Peninsula, both 2005 and 2012 episodes caused wide disturbances on ecosystems, with large areas showing water availability deficit in soils, driving to severe impacts on vegetation and productivity losses of ~ 40 TgC/year. Throughout Italy and Greece region, the events of 2003, 2007 and 2012 affected the ecosystems of about 30-35% of the territory, being 2007 particularly intense due to the combined effect of a drought, major heatwaves and large fires. In France, the 2006 episode affected more than 25% of the vegetation of the territory and induced losses on annual productivity of ~ 25 TgC/year. In turn, the occurrence of severe fire seasons is closely associated with the availability of biomass that easily burns in the presence of an extreme climatic event, such as summer heatwaves (e.g. Iberia in 2003 and 2017, and Italy and Greece in 2007), or persistent droughts in previous months (e.g. Iberia in 2005 and 2012, and Italy and Greece in 2012).

The assessment of the disturbances on photosynthetic activity caused by droughts and large fires allowed the quantification of the losses of vegetation productivity, and also, the evaluation of the recovery process during the following months. The ecosystems response varies widely, with vegetation may taking months to years to recover the normal activity. The disturbances on net productivity caused by droughts are significantly higher than the ones caused by large fires, especially due to their extension and their timescale, that can last from weeks to several months. However, despite fires have a shorter period of time, these events can strongly inhibit the vegetation to regenerate, amplifying the productivity losses on ecosystems during a long period.

Keywords: Droughts, Large Fires, Vegetation Recovery, Productivity Losses

Index

Table of Figures

List of Tables

List of Abbreviations and Symbols

APAR	Absorbed Photosynthetically Active Radiation
$A_{PIX_{i,j}}$	Pixel's area
BA	Burned Area
BPLUT	Biome Property Look-Up Table
C	Number of columns of grid
CL	Confidence Level
C_{LOSS}	Monthly Net Productivity Losses
CO_2	Carbon Dioxide
$dist_{lat}$	Length of pixels
$dist_{lon}$	Width of pixels
ε	Radiation Conversion Efficiency
EFFIS	European Forest Fire Information System
EMDAT	Emergency Events Database
ESA CCI	European Space Agency Climate Change Initiative
ET	Evapotranspiration
EUMETSAT	European Organization for the Exploitation of Meteorological Satellites
FPAR	Fraction of Photosynthetically Active Radiation
FR	France
GMAO	Global Modelling and Assimilation Office
GPP	Gross Primary Production
$GPP_{i,j}^{CLim}$	GPP Monthly Climatological Median 2001-2019
$GPP_{i,j,t}^{Anom}$	GPP Monthly Anomaly Fields
GtC	Gigatons of Carbon
ha	Hectares
IB	Iberian Peninsula
ICNF	Instituto da Conservação da Natureza e das Florestas
IG	Italy and Greece
IPAR	Incident Photosynthetically Active Radiation
IPCC	Intergovernmental Panel on Climate Change
JD	Julian Day
L	Number of lines of grid
LSA-SAF	Land Surface Analysis-Satellite Application Facility
LST	Land Surface Temperature
$medN$	Temporal Median of GPP (or SM) values for the N years
MODIS	Moderate Resolution Imaging Spectroradiometer
N	Number of years
NEON	National Ecological Observatory Network
PsNet	Net Photosynthesis
$PsN_{i,j,t}^{Anom}$	PsNet Monthly Anomaly Fields
SM	Soil Moisture
$SM_{i,j}^{CLim}$	SM Monthly Climatological Median 2001-2019
$SM_{i,j,t}^{Anom}$	Soil Moisture Monthly Anomaly Fields
$GPP_{i,j}^{std}$	Temporal Monthly Standard Deviation of GPP
RCP	Representative Concentration Pathways
TgC	Teragrams of Carbon
VPD	Vapour Pressure Deficit

1. Introduction

The dynamics of terrestrial ecosystems has been recurrently disturbed throughout the world, particularly due to the increasing occurrence of extreme events, as droughts and heatwaves (IPCC, 2018; Reichstein et al., 2013) which have direct effects on global ecosystem production estimates (Melillo et al., 1993). Europe, and in particular, the Mediterranean region, has been affected by several intense heatwaves and droughts in the last century, namely the mega heatwaves in 2003 over western Europe and in Russia during 2010 (Barriopedro et al., 2011; Bastos et al., 2014; Flach et al., 2018), or the Iberian droughts and their associated large fires (García-Herrera et al., 2007; Gouveia et al., 2012; Sánchez-Benítez et al., 2018). These events are frequently associated or compounded (Zscheischler et al., 2018), such as the 2003 and 2017 western European droughts and heatwaves associated with large fires in Iberia and France (Ruffault et al., 2018; Sánchez-Benítez et al., 2018) and the 2007 exceptional heatwave which triggered large fires on Italy and Greece, leading to the destruction of many hectares of forest (Gouveia et al., 2016; Koutsias et al., 2012). These episodes are thoroughly documented, mostly focusing on meteorological drivers of the events, but analysing, also, the magnitude and impacts on the ecosystems (Bastos et al., 2014; Gouveia et al., 2009, 2016).

The Mediterranean basin has been recognized as a hotspot region for the increasing frequency and severity of climatic extreme events (Grillakis, 2019; IPCC, 2018; Spinoni et al., 2018). According to the latest report of IPCC, some scenarios suggest a general decrease in annual mean precipitation that may be translated by a reduction of around 20-25% over the Mediterranean region, until the end of 21st century, leading to a dramatic shift on local vegetation dynamics and in carbon cycle (Del Grosso et al., 2008). Moreover, every year, fires destroy large parts of the ecosystems in the region, especially in the summer season (Pereira et al., 2005; Turco et al., 2017). The impact of these large fires on carbon cycle, and on released CO_2 towards atmosphere, is massive, because this area is highly vegetated, contributing not only to the increasing concentration of atmospheric CO_2, but also to the reduction of vegetation productivity, and other important nutrient stocks of soils and vegetation (Caon et al., 2014).

The terrestrial natural carbon cycle is composed by natural sources and sinks (Friedlingstein et al., 2019; Waring and Running, 2007). The carbon emissions are sources, which feed the carbon sinks, mainly represented by oceans, soils, atmosphere, and vegetation, able to take up the carbon dioxide through photosynthesis processes (Figure 1.1) (Friedlingstein et al., 2019). The oceans represent the major carbon reservoir, storing about ~38000 GtC, while, in land, soils store ~1500-2400 GtC, permafrost ~1700 GtC and vegetation ~450-600 GtC. The atmosphere also plays an important role on carbon sequestration, storing ~860 GtC. The gross uptake and release of carbon, between land-atmosphere and ocean-atmosphere, are almost balanced (120 GtC/year and 90 GtC/year, respectively) (Figure 1.1). Therefore, carbon is, on one hand, sequestrated and stored, and, on the other hand, is produced by a wide range of systems, through respiration and other natural activities, which release CO_2 into the atmosphere. Consequently, the mechanisms of emission and reduction are balanced, unless there is an internal or external forcing, which perturbates this balance (Falkowski et al., 2000).

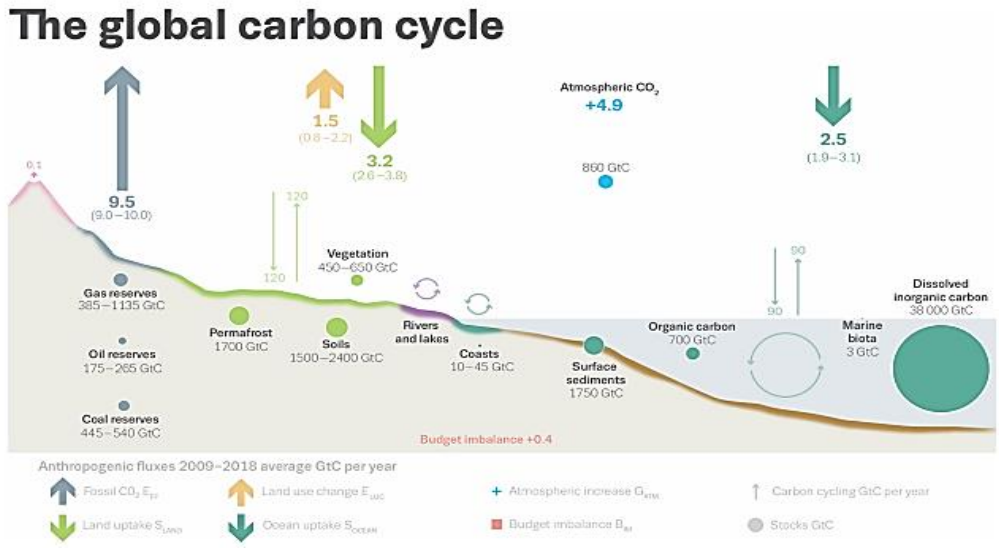

Figure 1.1 - Description of global carbon cycle: oceans represent the major carbon reservoir and, over land, soils are the major pool of carbon stored. The combustion of fossil fuels and the land use change have a large contribution to increase the amount of CO_2 on atmosphere by releasing 9.5 and 1.5 GtCO2/year. (Source: Friedlingstein et al., 2019).

Although the anthropogenic influence on the carbon cycle represents a small fraction of all intervening factors, the human related disturbances entail many consequences. Among those, the combustion of fossil fuels and land use change, which release, respectively, 9.5 $GtCO_2$/year and 1.5 $GtCO_2$/year to the atmosphere, are the most disturbing effects on carbon cycle (Friedlingstein et al., 2019; Mahowald et al., 2017), causing large losses on carbon stored, mainly in soils and vegetation. Dense forests have been intensively replaced, especially in highly populated regions, by urban areas, extensive agriculture, and diverse crops over the past years, leading to a decrease of local carbon sequestration by soils and, especially, by vegetation (Kaplan et al., 2012; Powers and Jetz, 2019).

The anthropogenic influence overpass local constrains and feedbacks and has a global impact in terms of global warming, being a reflection not only of changes in the mean global temperature, but also in the frequency, severity, and nature of extremes events (IPCC, 2018). Droughts and heatwaves breed high losses, both in terms of vegetation productivity and damages on ecosystems (Ciais et al., 2005; Flach et al., 2018), due to the strong temperature anomalies and lack of precipitation during a long period of time, inducing high soil moisture deficits and disturbances on regular photosynthesis and respiration mechanisms of soils and vegetation (Ballantyne et al., 2017).

Frank et al., (2015) concluded that, among the different types of extreme events (e.g. heatwaves, heavy precipitation or seasonal hurricanes and cyclones), droughts are the ones which are expected to have the major effect on carbon cycle. As a result, the carbon sink rates are affected, and the carbon uptake, made by ecosystems, weakens. Furthermore, besides the effects on vegetation, droughts can highly increase the risk of fires in the affected regions (Russo et al., 2017).

One key metric of carbon mass flux studies is Gross Primary Production (GPP), which represents the carbon assimilated through photosynthesis processes by the terrestrial ecosystems (Running et al., 2000). GPP constitutes a physical process to measure the conversion of carbon made by photosynthesis processes, and it can be modelled from satellite imagery (Turner et al., 2005, 2006). GPP highly depends on variables that are vulnerable to changes in climate, like soil moisture and temperature, and directly influences the evapotranspiration rates (Delworth and Manabe, 1988). Soil moisture is particularly important for the climate system because it influences the severity of extreme events on ecosystems (Martínez-Fernández et al., 2016), and, naturally, controls the vegetation development (Bolten and

Crow, 2012; Hirschi et al., 2011). GPP can be very useful to monitor the ecosystems conditions and production rates in the presence of an extreme event because it can capture, quantitatively, its impacts and, also provides the monitorization of the ecosystem's response (Bastos et al., 2014, 2020; Frank et al., 2015; Gouveia et al., 2012). The net photosynthesis (PsNet) quantifies the carbon that can be fixed through photosynthetic activity as the maintenance and respiration costs on leaves and roots are excluded, therefore corresponding to a balance between the plant production, described through GPP, and maintenance respiration costs (Running et al., 2004).

The relationship between climatic extreme and ecological response is not linear as the magnitude of the extreme climatic event may not imply an extreme response from the ecosystem (Smith, 2011). Hence, it is crucial to assess the role of different drivers, both climatic and biological, on vegetation dynamics. Moreover, the fact that the impacts of the climatic events on the ecosystems cannot be weighted only according their magnitude, should be accounted, as the response can occur during the event or can be lagged apart (Frank et al., 2015). Thus, it is extremely important to know, and understand the nature of the impact, to analyse the influence of the extreme event on the ecosystem and assess the correspondent response to comprehend the link between the climatological and biological variables, related with vegetation dynamics, in order to assess the ecological response.

This study aims to analyse how droughts and large fires affect the Mediterranean's vegetation productivity, by examining a set of severe episodes that occurred in three different regions (Iberian Peninsula, Italy and Greece, and France), between 2001 and 2019. The assessment of the persistence of dry conditions, combined with the observation of the number of months that vegetation's activity is disturbed, will allow to quantify the productivity losses, and comprehend the remarkable influence that the climatic extreme events have on vegetation's dynamics. Moreover, the present work intends to analyze the relationship between the severity of extreme events and the impacts caused on vegetation and its resilience to the events (vegetation response), by quantifying the lag time of ecosystems' recovery.

2. Data

2.1. Vegetation Satellite Products

The monitoring of global vegetation production can be performed using information obtained from different remote sensing instruments (e.g. MODIS, LSA-SAF products) or *in situ* data, through carbon tower fluxes (Helbig et al., 2017; Ueyama et al., 2013, NEON). Due to the irregular distribution of tower flux sensors within the study areas, the use of satellite information, which covers large and remote areas, and is now available for a large temporal window, is a valid alternative. Therefore, in this work, the option was to use the latter, allowing to assess the influence of climatic extreme events on vegetation dynamics (Gouveia et al., 2009). Moreover, the better spatial resolution of recent satellite products enables the evaluation of the responses of different biomes of vegetation. Therefore, the MODIS GPP product (MOD17A2), with 500m on original projection (sinusoidal), revealed to be the most appropriate satellite product for this study, encompassing both GPP and PsNet datasets.

GPP and PsNet products are daily cumulative composites of 8 days, expressed in kg C/m^2, for global spatial extent. The MODIS GPP product is based on Monteith's light use efficiency concept (Monteith, 1972) that considers different parameters, which have direct influence on the development of the plant and, in particularly, on photosynthesis. Hence, radiative parameters like radiation conversion efficiency, ε, and absorbed photosynthetically active radiation (APAR) need to be considered. The ε term is usually modelled by temperature variations and by the vapour pressure deficit (VPD) established between leaves and atmosphere - $\varepsilon(T, VPD)$. Therefore, the computation of the most approximate value of ε considers the maximum radiation efficiency (ε_{max}), parametrized by vapour pressure deficit (VPD), which directly depends on potential evapotranspiration, and the minimum temperature (T_{min}). These two factors are responsible for the attenuation of maximum efficiency so, it is essential to parametrize ε_{max} to obtain a better approach of real efficiency, ε, of specific type of vegetation.

Besides ε, Monteith's approach to compute GPP considers the photosynthetically active radiation (PAR) in the 0.4-0.7 [μm] spectral range (Rubio et al., 2005), determined by FPAR, which is the fraction of PAR absorbed by plant leaves, and IPAR, that corresponds to incident PAR on leaves. The combination of FPAR and IPAR originates the total absorbed PAR (APAR).

Based on the previous assumptions, Running et al., (2004) concluded that GPP estimation can be described through the combination of efficiency coefficient ε, which relies on temperature and vapour pressure deficit, and the absorbed photosynthetically active radiation (APAR) (Figure 2.1). Therefore, it can be ensured a good quality monitorization of a terrestrial ecosystem of any region of the globe, providing information about its efficiency production.

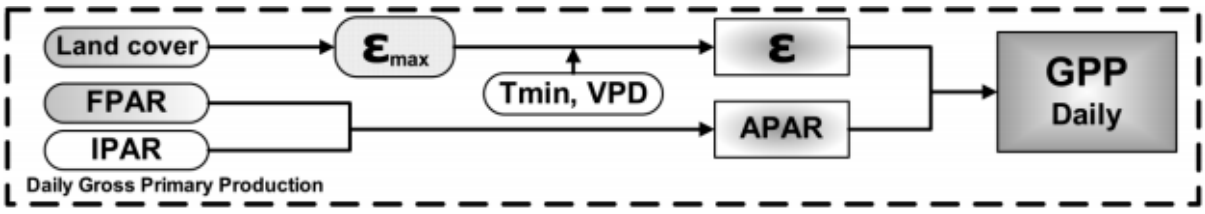

Figure 2.1 - MODIS GPP estimation (Source: Running et al., 2015)

The radiative parameters ε and APAR vary according to the different land covers and climate conditions of each region (White and Running, 1994). In specific permanent extreme conditions, the temperature values are higher and directly influences the VPD, by exacerbating its value. The establishment of this increasing gradient, between leaves and atmosphere, leads to stomata closure (Sippel et al., 2018). Therefore, these conditions disturb the photosynthetically activity, by reducing the efficiency ε, and consequently, the values of vegetation's production (GPP). Moreover, in hot and dry environments, the plants reduce the leaves' size, in order to decrease, especially, the transpiration rates and water losses (Sippel et al., 2018). This mechanism diminishes the leaves' surface availability to absorb radiation, which consequently reduces the photosynthesis activity, due to the variation on APAR, and naturally, the vegetation's production.

The changes go beyond photosynthesis processes when vegetation is under stress conditions. As the carbon allocation patterns responsible for the repair, maintenance, growth, and defence of the plant, are modified (Farooq et al., 2009), plants become more vulnerable to another stressors, like diseases or pests (Sala et al., 2012). Therefore, the productivity drastically reduces, and may enhance the risk of potential large fires that release the carbon stored on vegetation (biomass) towards the atmosphere, increasing the concentration of CO_2 (Flannigan et al., 2006).

The net photosynthesis (PsNet) dataset is also included in MOD17A2 product and corresponds to a balance between the plant production and plant maintenance. The plant production is assessed, and described, by GPP and the plant maintenance can be computed through the modelling of respiration's costs of leaves, $Leaf_{MR}$, and roots, $F_{Root_{MR}}$. This balance can be represented by the following equation (Running et al., 2004):

$$PsNet = GPP - Leaf_{MR} - F_{Root_{MR}} \tag{2.1}$$

Negative values of PsNet represent lower values of production than costs whereas positive values indicate higher values of production.

PsNet computation is dependent on a good discrimination of different landcovers. Therefore, to guarantee a higher accuracy (65 to 80%) of landcover description and allowing a better monitorization of global vegetation, it is assumed that there is no variation of biome-specific properties of an ecosystem at any time during the year (Friedl et al., 2010).

The spatial and temporal resolutions of both MODIS GPP and PsNet allow the evaluation of vegetation behaviour under climatic extreme conditions and, therefore, ensuring an accurate assessment of global terrestrial carbon cycle. In this study, the version 6 of MOD17A2 is used, that includes updates on global biome properties (BPLUT) description and on meteorological data (GMAO).

2.2. Soil Moisture

Accurate measures of soil moisture are complex and dependent on a wide range of variables, especially related with the different types of soil, and their physical characteristics, such as brightness temperature and dielectric properties. The measurement theory is based on microwave remote sensing work of Ulaby et al., (1982).

The European Space Agency Climate Change Initiative Soil Moisture (ESA CCI SM) has been recognized as a high-quality monitoring satellite product, useful for climate change and variability, with meteorological and hydrological applications, and land-atmosphere interactions studies (Casagrande et al., 2015; Dorigo et al., 2012, 2015; Liu et al., 2011). According to (Dorigo et al., 2017), which focus their study on the product validation, the average error variations of soil moisture on Europe are relatively low, and the fraction of days, per month, with valid observations, between 2001-2019, is higher than 50% for all the region, with an exceptional improvement from 2007 to 2019 (>70% for almost all months of the year). However, although ESA CCI SM shows a high accuracy values (Dorigo et al., 2017), the product limitations have to be accounted. According to the Soil Moisture ECV Product User Guide, vegetation affects the measurement, due to the implications on microwave emissions spectrum and, the denser the vegetation, less accurate are the estimations. Besides dense vegetation, the product show flaws on frozen surfaces and snow, waterbodies, and rainstorms during the satellite overpass because all these factors interferes with the microwave soil emissions, which are detected by the satellite. These limitations are described on a daily product dataset, named *flags*, which is used in this work in order to identify the regions where the soil moisture values can be defective. Each type of flaw is labelled with numbers to easily access the reason of the missing pixel value.

The ESA CCI SM product consists of three different datasets: active, passive, and combined. While the active product merges scatterometer instruments data from AMI-WS and ASCAT, which are aboard the EUMETSAT satellites, the passive product merges radiometer data derived from SMMR, SSM/I, TMI, AMSR-E, WindSat, AMSR2, and SMOS. Therefore, the combined dataset results of the combination of the different active and passive datasets.

In this work, the combined dataset is used, and it is described in volumetric units [m^3m^{-3}], available at global spatial extent, with a spatial resolution of 0.25° and a temporal resolution of 1 day.

2.3. Burned Areas

With the aim to describe the globally historical burned patterns, the MODIS Burned Areas Fire CCI version 5.1 (FireCCI51) was derived (Lizundia-Loiola et al., 2020), and the PIXEL product was adopted in this study to map the Burned Areas (BAs) over several regions within the study area.

FireCCI51 covers the period 2001-2019 and complement the previous version named FireCCI version 5.0 (Chuvieco et al., 2018) which, besides extending the temporal range, (previously from 2001-2016), also improves the algorithm to detect more accurately the BAs. This algorithm is described with more detail on Lizundia-Loiola et al., (2020).

FireCCI51 merges two MODIS satellite products: MOD09GQ Collection 6 and MCD14ML Collection 6. The first provides information associated with daily surface reflectance in the RED and NIR bands of MODIS Terra satellite, whereas the second offers thermal surface information. Therefore, the conjunction of these two variables (radiative and thermodynamic, respectively) can incorporate more information related with fires and respective BAs. Also, combined with its spatial resolution of 250m and monthly temporal resolution, this product shows high accuracy detection and monitorization of BAs.

The product is composed by three layers: the date of detection (Julian Day, hereafter JD), the level of confidence of the BA (Confidence Level, hereafter CL) and land cover in the pixel detected as burned. The JD corresponds to the day when the fire was firstly detected. Nevertheless, the date of burned pixel, sometimes, may not be coincident with the supposed burning date because it depends on image availability, the cloud coverage or the aerosols concentration around the BA. The CL corresponds to the probability of the pixel is burned. This layer is modelled through the analysis of uncertainty of the different input variables which were used in the MODIS BA algorithm (Lizundia-Loiola et al., 2020) and the measurement is based on the product's validation process of Padilla et al., (2018).

In this study, the JD and CL were used. The first layer is used in the detection of burned pixel while the second is used in order to assess the quality of detection of the burned pixel. The JD layer showed great accuracy in terms of confidence level of BAs detection according to the quality analysis made in this work, and this assessment is compared with all the detected pixels on CL dataset.

3. Methodology

Vegetation dynamics over the Mediterranean region is assessed through GPP and PsNet analysis, for a 19-year period, comprised between 2001 and 2019. Three different areas of the Mediterranean basin were analysed separately, in order to perform a deep analysis of the behaviour of the vegetation under extreme events (droughts or fires) on each of the areas, namely the Iberian Peninsula (hereafter IB), Italy and Greece (hereafter IG) and France (hereafter FR) (Figure 3.1).

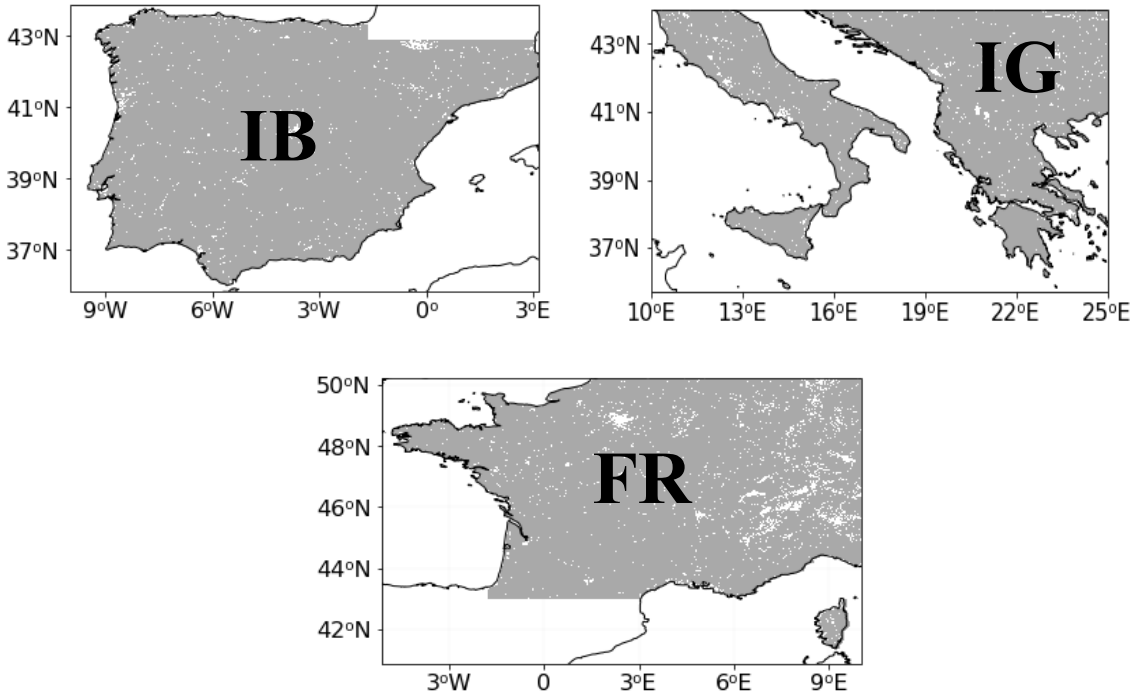

Figure 3.1 - Study Areas: Iberian Peninsula (hereafter IB), Italy and Greece (hereafter IG) and France (hereafter FR).

3.1. GPP and SM Anomaly Fields

Drought events are expected to last several weeks to months, or even, in extreme cases, years. Their impacts on vegetation, which shift its regimes and dynamics, also vary, depending on the extreme event's duration. As described on section 2.1. and 2.2., GPP information is provided as an 8-day cumulative composite, while SM is disseminated daily. Considering that the duration of the common drought events in Mediterranean region is lower than one year, GPP monthly fields were computed, corresponding to the cumulative sum of every week of each month. Related to SM, since this variable presents rapid fluctuations, closely associated with precipitation regimes, weekly fields of SM were used, corresponding to the weekly mean value. However, it is important to stress that SM data showed some drawbacks, especially during autumn and winter months, due to the increasing frozen surfaces along the study areas. Consequently, in order to obtain more accurate results, for every week, the weekly mean value was computed only for the pixels which had 5 or more days of a week of data, and the pixels of SM grid which had less than 5 days of information were masked.

In order to obtain the anomaly fields of both variables, it was necessary to determine, firstly, the climatological medians for each latitude and longitude point of the grid (i, j). The equations used to obtain the monthly climatological median of GPP ($GPP_{i,j}^{Clim}$) and weekly climatological median of SM ($SM_{i,j}^{Clim}$), considering the period 2001-2019 (N=19 years) for the LxC grid pixels, were:

$$GPP_{i,j}^{Clim} = medN\left(GPP_{i,j,t}\right), t = 1, \dots, N \tag{3.1}$$

$$SM_{i,j}^{Clim} = medN\left(SM_{i,j,t}\right), t = 1, \dots, N \tag{3.2}$$

where $medN$ represents the temporal median of GPP and SM values and L,C represent the number of lines and columns, respectively, of each study area grid.

Afterwards, monthly GPP and weekly SM anomaly fields ($GPP_{i,j,t}^{Anom}$ and $SM_{i,j,t}^{Anom}$) were determined for each LxC pixels, as described on equations 3.3 and 3.4, respectively. The monthly GPP and weekly SM anomaly fields are computed as departure from the climatological medians defined by equations 3.1 and 3.2.

$$GPP_{i,j,t}^{Anom} = GPP_{i,j,t} - GPP_{i,j}^{Clim} \tag{3.3}$$

$$SM_{i,j,t}^{Anom} = SM_{i,j,t} - SM_{i,j}^{Clim} \tag{3.4}$$

The information provided by the SM anomaly fields, combined with the vegetation's anomalies of GPP, is helpful to characterize and to observe the driest periods with high soil moisture deficits, which induced severe disturbances on ecosystems, between 2001 and 2019, over the Mediterranean region.

The statistical computation of the 25th percentile for SM anomalies over each LxC pixels enables to distinguish the months, and the regions, whose SM anomaly fields are characterized by stronger deficits, and to identify the areas which had more potential ecosystem damages due to extreme events over the 2001-2019 period.

In terms of GPP statistical analysis, the computation of monthly standard deviation can be very useful to understand the spatial and monthly variability patterns of vegetation's productivity during the study period. Moreover, it allows the observation of the periods whose vegetation has more activity, characterized by higher median values, which are, for the Mediterranean ecosystems, the months between April and October, as depicted on Figure A.1 of Appendix.

3.2. Droughts and Burned Areas

With the aim of determining the drought episodes with the highest impact on different regions of Mediterranean, a regional GPP anomaly threshold is established for each one of the areas represented on Figure 3.1. This threshold is a key factor of this work because enables the selection of the vegetated areas which were affected by a drought and excludes the ones which were not affected or showed ability to resist to the specific extreme event.

The definition of each area's threshold is based on GPP variability analysis, statistically assessed through the temporal monthly standard deviation, as described on equation 3.5:

$$GPP_{i,j}^{std} = std\left(GPP_{i,j,t}\right), t = 1, \dots, N \quad (3.5)$$

As mentioned on section 3.1, the temporal standard deviation of GPP is computed for each area, between April and October (months with more vegetation activity), throughout the study period. Then, the spatial mean of GPP standard deviation of all the grid pixels, of each area, is computed, in order to define the value of the threshold. Naturally, since the dynamics of the vegetation varies throughout the study areas, the mean of the standard deviation will, also, be different for each region, defining, consequently, a different anomaly threshold for the three regions. The value of each region threshold is described on Table 3.1.

The definition of drought for this work, following the methodology from Gouveia et al., (2009, 2012), is based on the persistence of vegetation stress conditions. The analysis relies on the number of months, for every year, between April and October, that has showed GPP monthly anomalies lower than the specific regional threshold. Then, the pixels on each of the studied regions which had three, or more months (of a total of seven) with GPP anomalies below the regional threshold, are classified as under drought conditions.

The choice of three or more months (out of seven) is based on the fact that droughts last, generally, several weeks. It is important to stress that, the definition of drought in this work does not distinguish the low values of productivity caused by external factors like diseases or pests, and also, does not discriminate between the type of extreme event which struck the region, like a heatwave, a drought or a large fire or the simultaneous co-occurrence of these events (Flach et al., 2018; Zscheischler et al., 2018).

Based on the applied methodology, the years when droughts' impacts are the highest on each area's vegetation are described on Table 3.1., together with the value of GPP anomaly threshold of each area and the extension of the vegetation impacts of the climate event, in percentage and km^2.

Table 3.1 - Values of each region threshold for GPP anomaly values and the years with the most drought areas with the correspondent affected area, in % and km2.

	GPP THRESHOLD	YEARS	AFFECTED AREA [%]	AFFECTED AREA [km^2]
IB	-0.0178	**2005**	42.83	250 712
		2012	25.34	147 217
IG	-0.0237	**2003**	33.62	143 976
		2007	35.89	153 905
		2012	30.44	129 768
FR	-0.0249	**2006**	27.34	178 629

The affected areas, presented on Table 3.1, are determined by computing the product between the number of pixels disturbed by the event, and the correspondent area of the pixel. As mentioned on section 2.1., the spatial resolution of vegetation data is 500m, with sinusoidal projection. However, in order to allow a better manipulation of data, the vegetation grid is reprojected, from sinusoidal to geographic projection. Therefore, the initial size of pixels is going to change, being necessary to assess the new size of each pixel.

The computation of the pixel's size in a geographic projection considers the latitudes and longitudes from the study region. It is known *a priori* that, in this context, the value of one degree of latitude is, in every point of the globe, 111.12 km. However, the longitude value varies with the cosine of latitude, being maximum on equatorial region, where latitude is zero, and null on the poles, where the latitude is 90º. Hence, the length of the pixel is computed, using the following equation:

$$dist_{lat} = 111.12 \times \left(lat_{i,j} - lat_{(i,j)+1}\right) \tag{3.6}$$

The $dist_{lat}$ is always the same for the i,j pixels, as expected, due to the regular grid of the projection. By applying the equation 3.6, it can be ensured that the computation of the length of the pixel through the latitude is equal for every pixel.

The parameter, which has variation on each point, is the width of the pixel, determined by longitude. Following the next equation, the width of the pixels is:

$$dist_{lon} = dist_{lat} \times cos\left(lat_{i,j}\right) \tag{3.7}$$

The cosine parameter varies from point to point due to the variation of latitude parameter. Consequently, the LxC pixel's area, given by the product between $dist_{lat}$ and the correspondent $dist_{lon}$, decreases northwards.

There is a wide range of documentation that assess the years with highest BAs over the Mediterranean region, namely on Iberia (Trigo et al., 2006; Gouveia et al., 2012; Turco et al, 2019), Greece (Koutsias et al., 2012; Gouveia et al., 2016) or France (Ruffalt et al., 2017). Besides mentioned bibliography, the information related with Mediterranean fires relies on annual EFFIS reports (https://effis.jrc.ec.europa.eu/reports-and-publications/annual-fire-reports).

On Table 3.2, it is possible to observe the years, between 2001 and 2019, with more BA over each study region. The information, extracted from EFFIS reports, is divided according the three chosen regions, already defined, and the countries which are part of each study area. The values on bold indicates, for each area, and the respective country, when the BAs were above 1980-2019 average value of the country, indicating a study case.

Table 3.2 – Burned area during the years with the highest BAs on study region, between 2001-2019. The value of BAs is compared to the average (1980-2019) for each country which integrates the study area. The value on bold indicates that the BA was above the 1980-2019 average (Source: EFFIS annual reports).

	Burned Area [ha]				
	IB		*IG*		*FR*
	Portugal	**Spain**	**Italy**	**Greece**	**France**
2003	**421 835**	149 224	91 803	3 397	**74 000**
2005	**338 262**	**179 929**	47 575	6 437	17 356
2007	31 450	82 048	**227 729**	**225 734**	8 570
2012	110 231	**209 855**	**130 814**	**59 924**	8 600
2017	**540 630**	**178 234**	**137 103**	13 393	**26 378**
Average (1980-2019)	*115 024*	*156 962*	*103 377*	*42 496*	*24 182*

The BAs of critical years for each box are assessed through JD dataset, integrated on Fire CCI data (described on section 2.3). A careful analysis of JD level of confidence is made, through CL dataset considering all pixels, with the aim to analyse the confidence level of those pixels, but also, to compare JD BA patterns of the critical years, with documented reports, provided by EFFIS specific report of each country.

The fire activity season is generally comprised, for the Mediterranean region, between June and October. Although in some of these years the fire season could had started earlier or finished later, for this analysis, the months outside this specific period are excluded.

The following Table 3.3 describes the extension of detected BAs, in percentage and km^2, of the selected years previously described on Table 3.2.

Table 3.3 – Area affected during the severest fire seasons of each study region in percentage of affected territory area (%) and km^2.

	YEARS	AFFECTED AREA [%]	AFFECTED AREA [km^2]
IB	**2003**	1.27	7 304
	2005	0.95	5 448
	2012	0.41	2 332
	2017	1.26	7 177
IG	**2007**	2.72	11 726
	2012	2.12	9 081
	2017	1.59	6 739
FR	**2003**	0.13	807
	2017	0.04	279

3.3. Net Photosynthesis Assessment

The impact of droughts and fires on vegetation, and the quantification of net photosynthesis disturbances due to extreme events can be evaluated through PsNet analysis (Bastos et al., 2014). The PsNet monthly values are computed using the same methodology of GPP (equation 3.1), as well as the monthly anomaly values, $PsN_{i,j,t}^{Anom}$ (equation 3.3), considering the monthly climatological median of 2001-2019.

The identification of burned pixels is performed using the method described on section 3.2, and then, PsNet evolution on time is assessed. The JD fires data, with 250m of spatial resolution, are resampled to the same spatial resolution of PsNet data, applying the nearest neighbour interpolation technique.

The first step on the assessment of vegetation's dynamics consists on the computation of PsNet monthly accumulated values on affected pixels for each of the selected years (described on Table 3.1) for each region. This process is determined for the year of the occurrence of the extreme event and for the following two years, in order to observe the vegetation's recovery after the event. Besides monthly

PsNet accumulation, the monthly mean anomalies are determined, in order to analyse the monthly pattern of vegetation productivity anomalies over the region.

The net photosynthesis disturbances occurred in each study case is assessed through the computation of monthly, and yearly losses of vegetation productivity. The monthly losses, C_{LOSS}, correspond to the sum of the product between monthly PsNet anomaly fields ($PsN_{i,j}^{Anom}$) of LxC affected pixels and the correspondent pixel area ($A_{PIX_{i,j}}$), based on the array of LxC pixel's area already computed. Therefore, the C_{LOSS} can be described by the following equation (3.8):

$$C_{LOSS} = \sum_{i=1}^{L}\sum_{j=1}^{C} PsN_{i,j}^{Anom} \cdot A_{PIX_{i,j}} \tag{3.8}$$

The yearly productivity losses are straightforward to determine, corresponding to the sum of all monthly C_{LOSS} . The units are kg C/year and kg C/month, respectively. The methodology applied to determine the dynamics of photosynthesis (PsNet) and the productivity disturbances, associated to droughts and fires, is the same.

The yearly disturbances allow the quantification of the net productivity losses, relatively to median, during the year in which extreme event occurred, and in the following two years. It should be noted that for the large fires' analysis, the yearly balance of the year occurrences only includes the months between June and December, in order to perform the burned vegetation productivity from the beginning of the fire season.

The vegetation's recovery definition, or the vegetation response, described in this work is related to the ending of the period of drought impact on vegetation, and corresponds to the moment when the values of GPP and PsNet achieved a similar magnitude to the median historical values.

4. Results and Discussion

4.1. Characterization of SM deficits and GPP anomaly fields

4.1.1. Iberian Peninsula (IB)

Table 3.1 highlights the years of 2005 and 2012 as the years with larger area whose vegetation was under dry persistent conditions over IB, being 2005 the year of the study period (2001-2019) with the largest area with GPP anomalies below the regional anomaly threshold.

The vegetation of the western area of IB was particularly affected during the 2005 drought episode (Figure 4.1, top left panel). The extension of this climatic extreme event on ecosystems was clearly remarkable, affecting 42.83% of the region (250 712 km^2) (Table 3.1). The impacts seem to occur with more incidence on vegetation of the southwest and western sectors, and also on northeast territories, showing large areas with 3 to 6 months of persistent below-average productivity (Figure 4.1, top right panel). These results completely agree with Gouveia and co-authors analysis of drought persistence on Portugal and Iberia in 2005 (Gouveia et al., 2009, 2012).

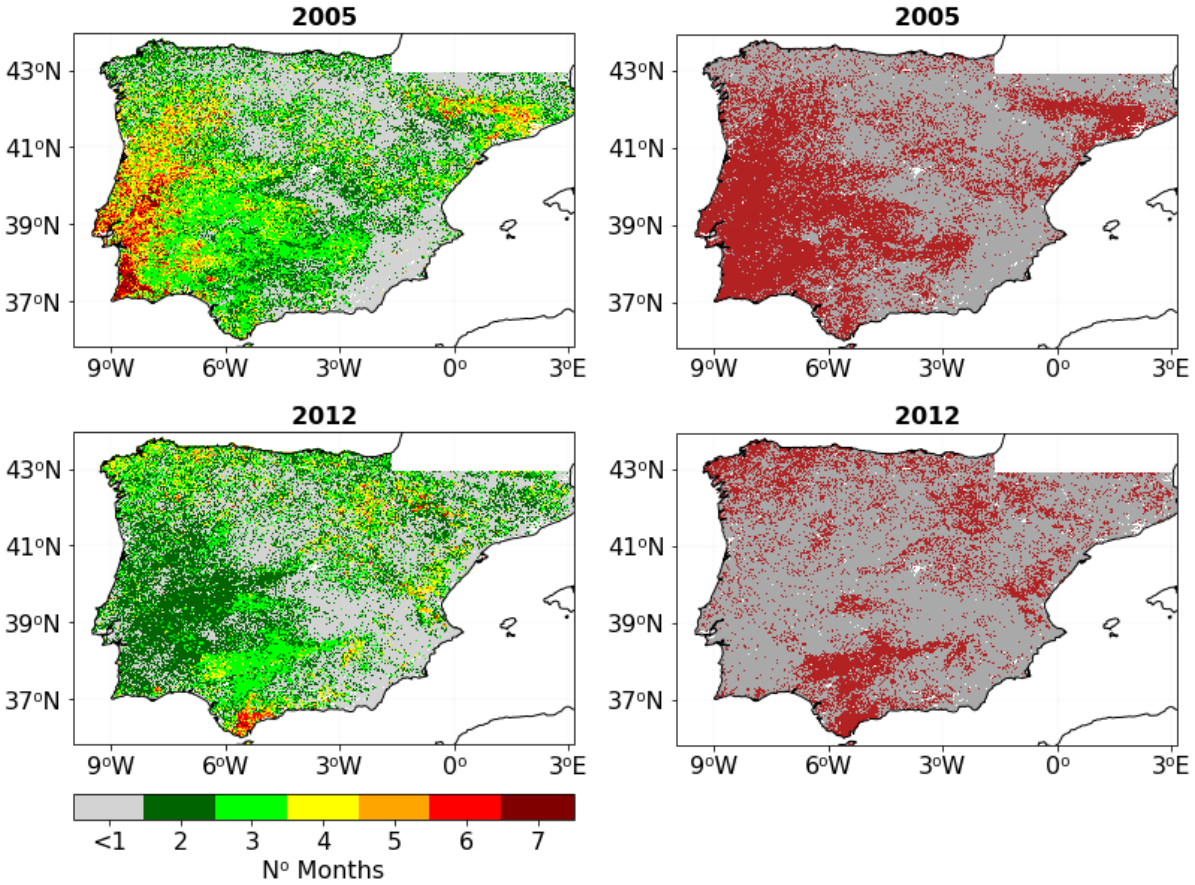

Figure 4.1 – Number of months on IB, between April and October, showing GPP anomalies below the threshold (left panels) and selected pixels affected by the impacts of droughts (right panels), during 2005 (top panels) and 2012 (bottom panels).

The SM results for 2005 (Figure 4.2, blue line) denote high SM deficits between January and March and between May and September, with the 25th percentile of anomalies value fluctuating between -0.02 and -0.05. These deficits seem to be related with the negative anomalies of GPP, since the vegetation highly depends on water soil availability.

During 2012, the affected areas, mainly located on the northwest and the south regions of IB, showed about 3 to 4 months of negative GPP anomalies below the threshold, with some scattered points exhibiting up to 5 months and the region of Malaga presenting up to 6 months (Figure 4.1, bottom panels).

The late months of winter, and the beginning of spring of 2012, were particularly dry (Figure 4.2, red line), especially during February when the value of 25th percentile of SM anomalies reached ~ -0.12. Despite the increasing of 25th percentile values during late spring, it was still expected an intense impact on vegetation dynamics over this period, as the effects of winter drought being slightly reduced due to the relatively wet late spring, when SM 25th percentile was fluctuating between -0.03 (April) and +0.01 (May). Otherwise, the impacts could be quite hazardous during summer if the spring months did not have higher values of precipitation.

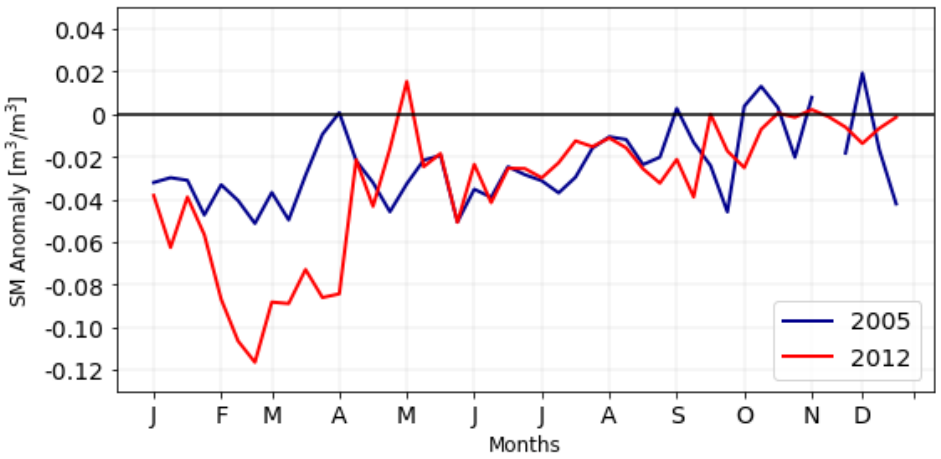

Figure 4.2 - Annual variations of 25th Percentile of SM anomaly values on IB, during 2005 and 2012.

In summary, the drought events of 2005 and 2012 correspond to the years which contributed the most to the disturbances on vegetation productivity throughout IB. However, 2005 was more severe than 2012, in terms of vegetation disturbances, with more affected areas for a longer number of months.

4.1.2. Italy and Greece (IG)

The years of 2003, 2007 and 2012 are the three years that showed the highest disturbances on vegetation, between 2001-2019, over IG region (Table 3.1). Particularly, 2003 episode was especially critical on ecosystems of the Italian territory and western Greece, affecting 143 976 km^2 (33.62% of IG territory, Table 3.1), with GPP anomalies ranging from 3 to 5 months below the regional anomaly threshold (Figure 4.3, top right panel).

The 2007 drought event affected 153 905 km^2 of IG ecosystems (35.89% of total area, Table 3.1), representing the year with the highest affected area during the study period. The Italian and Greek territories, especially the Peloponnese Peninsula, were quite disturbed, revealing 3 to 5 months of productivity below the regional anomaly threshold and, in some localized spots, reached 6 to 7 months (Figure 4.3, middle left panel). Besides Italy, the Balkans were, also, severely affected by the 2007 drought.

IG ecosystems were also stricken by a severe drought event during the year of 2012, with 30.44% of territory affected by GPP anomalies below the threshold (129 768 km^2, Table 3.1) (Figure 4.3, bottom left panel).

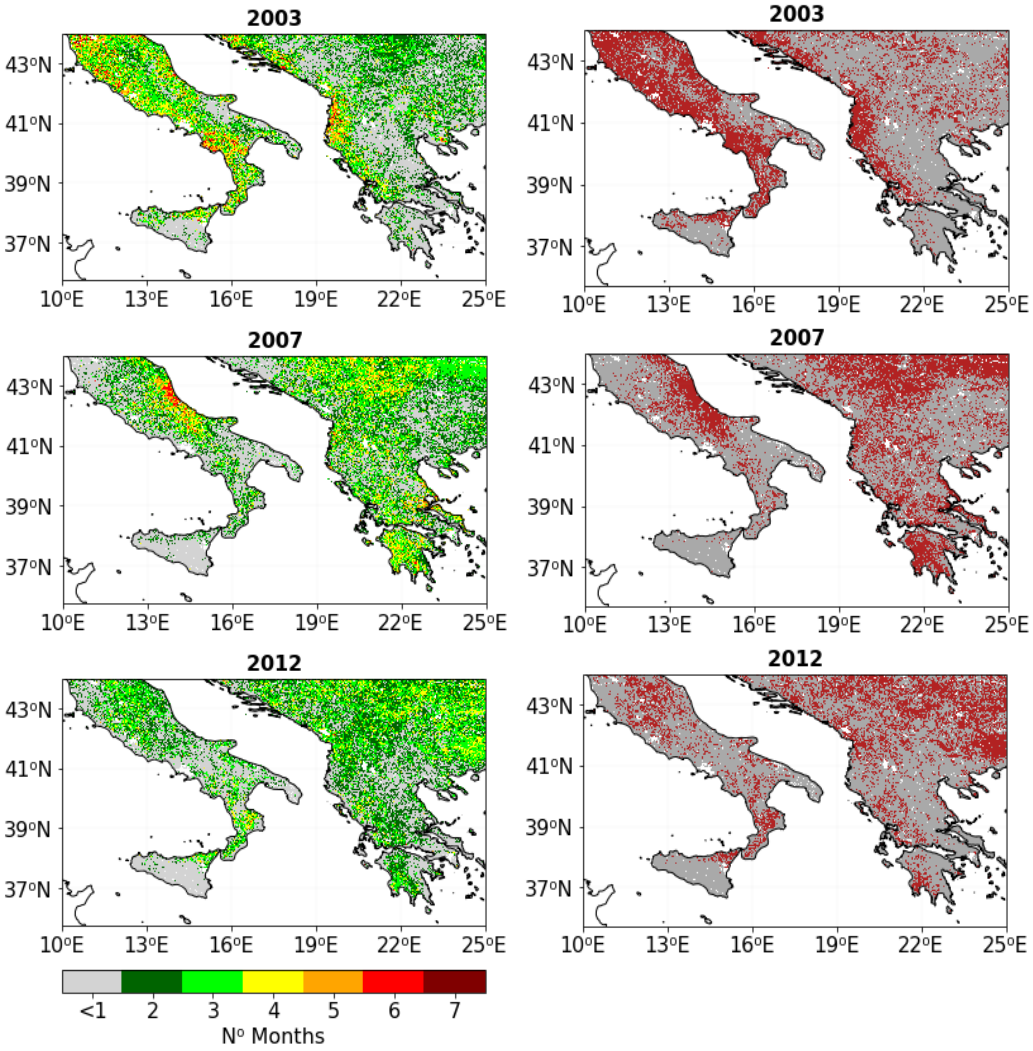

Figure 4.3 – As in Figure 4.1, but respecting to IG for 2003 (top panels), 2007 (middle panels) and 2012 (bottom panels).

During 2003, the IG 25th percentile of SM anomalies (Figure 4.4, blue line) reached -0.08 in February, and persisted strongly negative during spring and summer seasons, fluctuating between -0.02 and -0.06, indicating the persistence of the extreme event.

The drought conditions of 2007 episode can be supported by looking to SM results (Figure 4.4, red line). During spring, the SM 25th percentile changed between -0.04 and -0.01 and its value persisted strongly negative until September, reaching -0.06 in July.

In 2012, the disturbances on vegetation, described on Figure 4.3 (bottom panels), can be strongly supported by SM results (Figure 4.4, green line). The 25th percentile of SM anomalies was negative during almost the year, except during some weeks in April and May. The late winter, as well as the summer, were quite dry because the 25th percentile value was below -0.02 and, in some occasions, reached -0.04/-0.05 during July and August. Since the IG soils were quite dry during almost the year, it is expected to observe strong perturbations on GPP of vegetation.

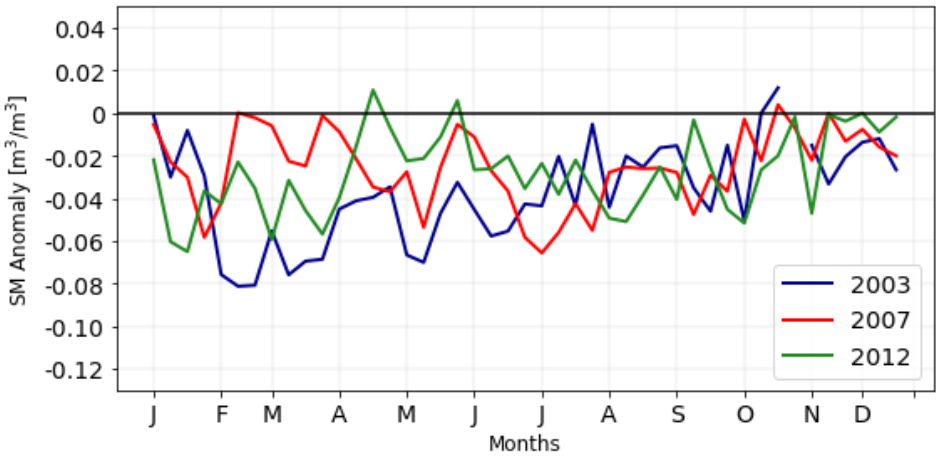

Figure 4.4 - As in Figure 4.2, but respecting to IG during 2003, 2007 and 2012.

4.1.3. France (FR)

The impacts on ecosystems of drought events during the period 2001-2019 affected mostly the southern and central areas of FR, especially 2003 and 2019 events. The remarkable drought episode occurred in 2003 (Bastos et al., 2014) had a strong impact on vegetation, mainly over southern France and Corsica, corresponding to ~16% of the study area. Due to its more localized impacts, and although its severity, this event is not considered here as a study case. Over FR region, the only year that disturbed more than one fourth of the vegetation of this study area was 2006 (178 629 km^2, Table 3.1). The influence of this extreme event on vegetation spread throughout the FR territory (Figures 4.5) being the only episode analysed in this area.

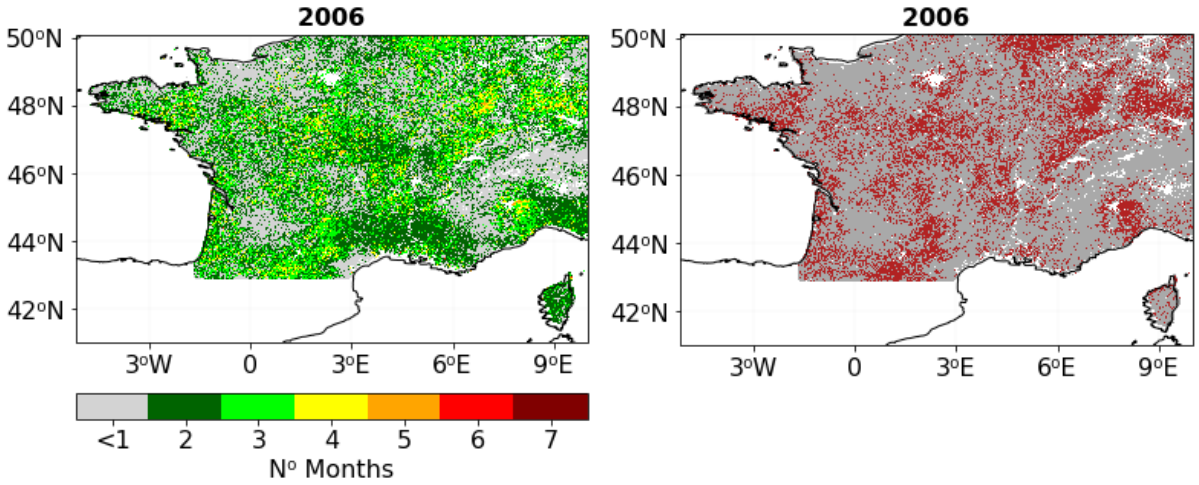

Figure 4.5 – As in Figure 4.1 but respecting to 2006 drought over FR region.

Drought conditions were persistent during the 2006 winter, namely between January and March, as depicted by the 25th percentile of SM anomalies varying between -0.04 and -0.01 (Figure 4.6). However, the occurrence of a slightly wet spring, depicted by the positive 25th percentile, possibly decreased the effects of drought.

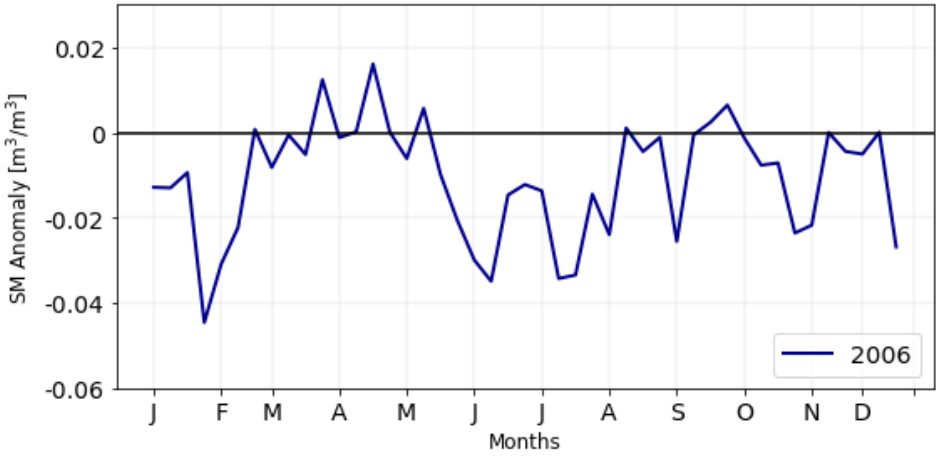

Figure 4.6 – As in Figure 4.2 but respecting to FR region in 2006.

4.2. Impact of Droughts on Vegetation Net Photosynthesis

4.2.1. Iberian Peninsula Drought Events

As mentioned before, GPP was severely influenced by droughts during the episodes of 2005 and 2012, with strong impacts on photosynthesis over the IB region.

The drought event of 2005 had a clear negative impact on net photosynthesis, as shown by the accumulated values of PsNet (red line in Figure 4.7, left panel) that are far below the 2001-2019 median (dashed blue line) of the selected pixels (0.635 vs. 0.796 kg C/m^2/month). Although the low photosynthesis activity typical of the winter months, the disturbances on PsNet are quite evident during the first three months of the year. These results are in good agreement with previous authors which pointed out the beginning of the 2005 event in the 2004 fall (García-Herrera et al., 2007; Gouveia et al., 2009, 2012). Furthermore, during the spring and summer seasons, the vegetation productivity decreased, as depicted on the lower monthly PsNet anomalies between March and June (Figure 4.8, left panel).

The recovery of vegetation after the 2005 drought event may not have occurred in 2006, as depicted on Figure 4.7 (light green line, left panel), with the 2006 PsNet accumulated values (0.743 kg C/m^2/month) showing that the vegetation was quite inhibited to recover from drought. According to EMDAT, a heatwave struck IB region in July 2006, and lasted approximately two weeks. Therefore, the regeneration process seems to occur delayed, not only due to the massive disturbances with origin on the extreme drought event, but also due to the 2006 summer heatwave. These results are in good agreement with Figure 4.8 (left panel) that shows slightly negative anomaly values of PsNet monthly mean over the affected pixels during winter and spring months, except in April, and strong negative anomalies in summer months.

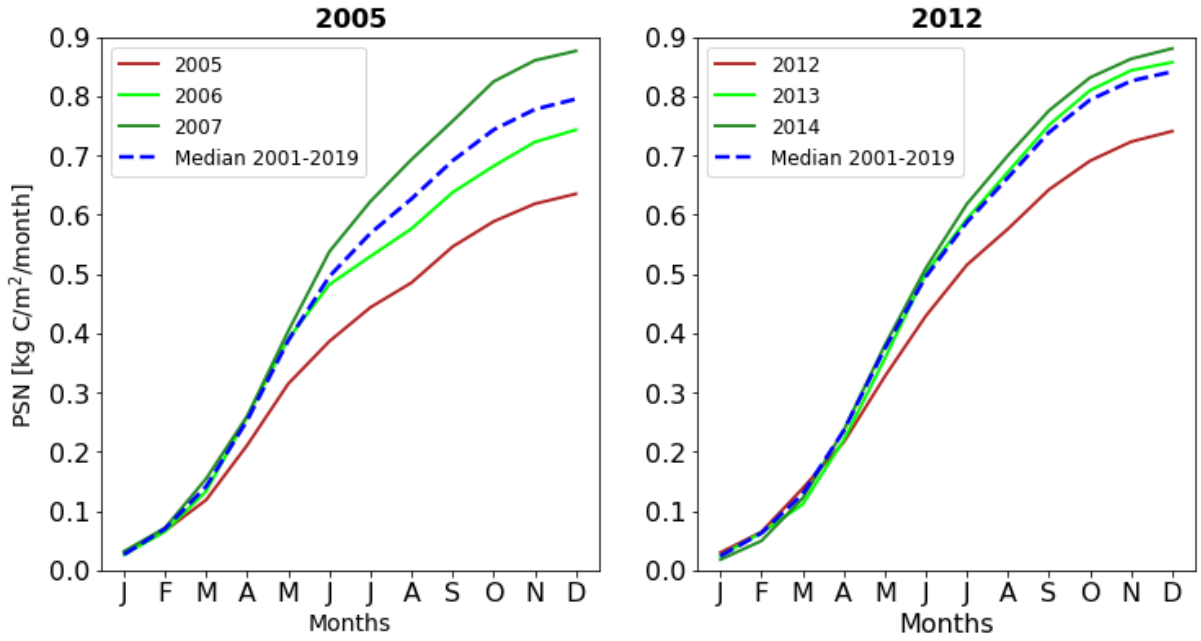

Figure 4.7 – Accumulated PsNet on IB for the considered affected pixels during the year of drought (red) and the two following years of recovery (light and dark green) (2005 on left panel and 2012 right panel). The accumulated historical median 2001-2019 of drought affected pixels is depicted by the blue dashed line.

The regeneration of vegetation activity occurred in 2007, with higher accumulation (0.876 kg C/m^2/month) and positive monthly mean anomalies of PsNet (Figures 4.7 and 4.8, left panels). However, it should be stressed that the high photosynthesis activity during 2007 does not compensate all the strong anomalies that occurred on vegetation photosynthesis during 2005 and 2006 (Figure 4.8, left panel).

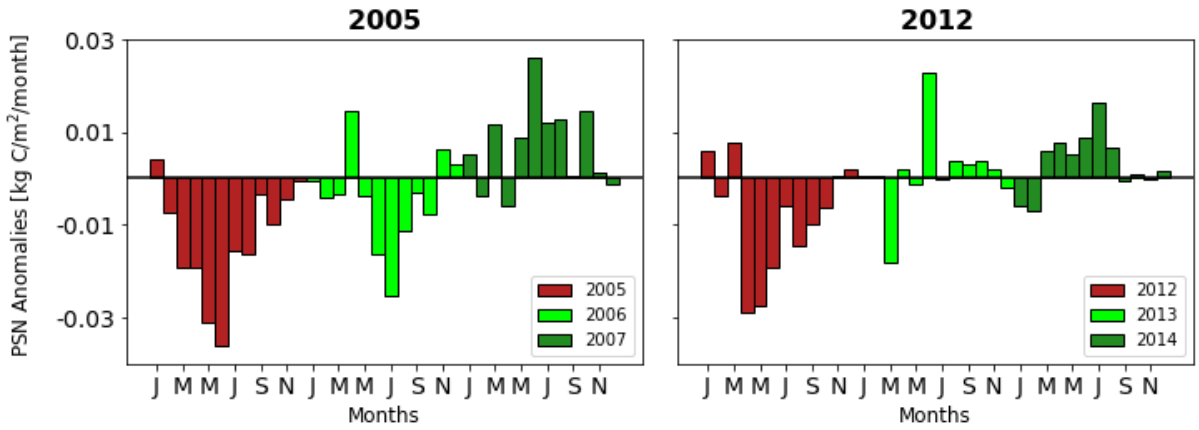

Figure 4.8 – Averaged PsNet monthly anomaly values over selected pixels during the drought year (red) and the following two years (light and dark green) for the drought episode of 2005 (left panel) and 2012 (right panel) over IB region.

According to Table 4.1, the losses on annual productivity were higher than 40 TgC/year in 2005, with all months, except for January, registering large disturbances, which clearly evidence that 2005 IB drought was truly remarkable and had a tremendous impact on ecosystems activity. During 2006, the yearly net photosynthesis balance was negative (-12.96 TgC/year), may be due to the summer heatwave, while 2007 showed a strong positive balance (+20.28 TgC/year), indicating some recovery of IB vegetation from the extreme events that occurred in 2005 and 2006.

Table 4.1 - Quantification of net photosynthesis disturbances, with monthly and yearly balances for 2005 and 2012 IB droughts. The monthly values are described on TgC/month and the yearly balance is described on TgC/year.

NET PHOTOSYNTHESIS LOSSES IB - 2005 AND 2012 DROUGHTS

	J	F	M	A	M	J	J	A	S	O	N	D	**TOTAL**
2005	1.02	-1.87	-4.92	-4.86	-7.90	-9.14	-3.89	-4.10	-0.90	-2.44	-1.14	-0.19	**-40.33**
2006	-0.13	-1.03	-0.86	3.65	-1.03	-4.05	-6.27	-2.85	-0.75	-1.97	1.53	0.80	**-12.96**
2007	1.34	-0.94	2.92	-1.54	2.25	6.49	2.92	3.16	0.12	3.64	0.30	-0.38	**20.28**
2012	0.86	-0.56	1.07	-4.29	-4.12	-2.88	-0.88	-2.13	-1.45	-0.93	0.06	0.30	**-14.93**
2013	0.05	0.07	-2.69	0.31	-0.09	3.36	-0.04	0.55	0.43	0.56	0.26	-0.30	**2.47**
2014	-0.89	-1.06	0.88	1.15	0.73	1.25	2.39	0.93	-0.06	0.15	-0.02	0.26	**5.71**

In the case of 2012 episode (red line), the accumulation of PsNet on drought affected pixels (red line) is far below the median 2001-2019 (dashed blue line) (0.741 vs. 0.843 kg C/m^2/month) (Figure 4.7, right panel). As seen previously, SM results pointed out that the late winter and the early spring of 2012

were dry whereas spring season was wet. However, the PsNet results show that, despite the water availability on soil during 2012 spring, the vegetation could not adapt to the strong soil water deficit occurred in winter. Therefore, the consequences lasted for the following months, disturbing the vegetation's production rates on spring and on summer, as described on Figure 4.8 (right panel), with strong negative PsNet monthly anomalies between April and October of 2012.

The ecosystems recovery to the 2012 extreme drought event occurred during the following years, as depicted on Figures 4.7 and 4.8 (right panels). The accumulated PsNet values of 2013 (light green line) are slightly higher than historical median (0.857 kg C/m^2/month), and during 2014, the accumulated values (dark green line) are higher than the median (0.880 kg C/m^2/month). The Figure 4.8 (right panel) highlights that, after vegetation's photosynthesis activity of IB reached a sequence of strong negative anomalies in 2012, especially during spring and summer, the recover process slowly started in 2013 spring season, and became more intense in 2014, with more than 75% of year presenting positive monthly anomalies of PsNet.

The year of 2012 revealed, as expected, a below-average annual net productivity balance, with losses of ~15 TgC/year that occurred, mainly, during the spring season (Table 4.1). The vegetation recovery from 2012 drought was weak, with 2013 ending with a balance of +2.47 TgC/year and 2014 ending with +5.71 TgC/year. Therefore, although both years had positive yearly values, the ecosystem response was not enough to cover all the losses that occurred during the 2012 drought.

It should be noted that, despite the different disturbed areas by 2005 and 2012 droughts, as well as their extension and, possibly, the different types of land cover affected by each extreme drought episode, the PsNet accumulation during 2012 is clearly higher than in 2005 (0.741 on 2012 vs. 0.635 kg C/m^2/month, on 2005), which reinforce the severity of the 2005 drought episode. Therefore, it seems that the response to the extreme event is quite different in each year and, the vegetation affected during 2012, despite the high deficit of water availability in late winter and early spring, had a better, and resilient response, than the local vegetation perturbated during 2005. These results allow to corroborate the Smith (2011) hypothesis, demonstrating that a climatic extreme event does not properly imply an extreme response of ecosystems.

4.2.2. Italy and Greece Drought Events

The accumulated values of PsNet during the three selected years over IG are shown on Figure 4.9. Over the affected pixels by the 2003 drought (red line, Figure 4.9, left panel) the values are quite below the historical median 2001-2019 (blue dashed line) (0.794 vs. 0.944 kg C/m^2/month). The disturbances had their takeoff between April and May and strongly accentuated during summer months. The strong vegetation productivity deficits can be highlighted by the monthly anomalies that remained negative 17 consecutive months (January 2003 to May 2004) (Figure 4.10, left panel).

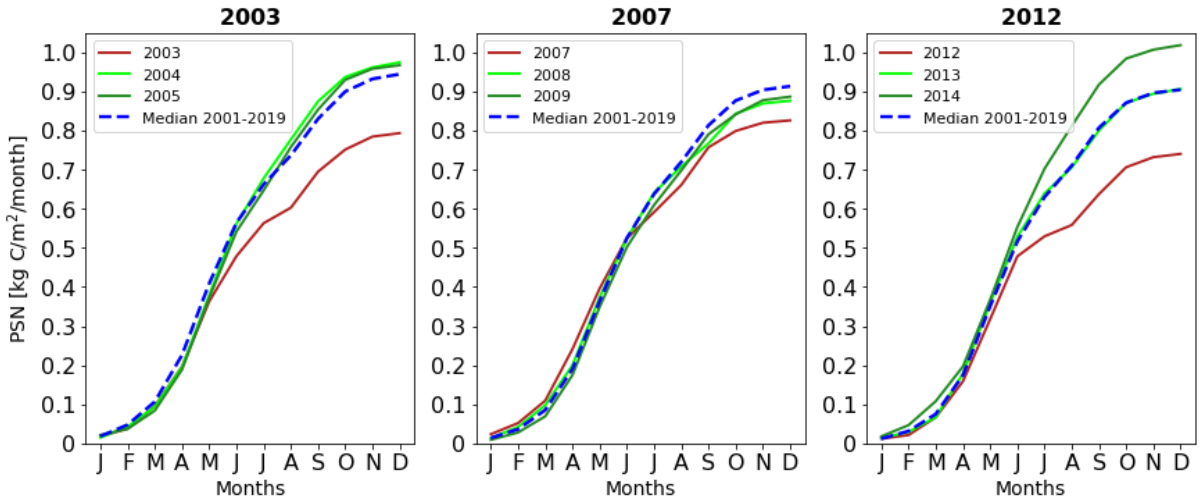

Figure 4.9 - As in Figure 4.7, but respecting to IG region for 2003 (left panel), 2007 (central panel) and 2012 (right panel).

The ecosystem recovery of the 2003 drought's affected regions started to occur in the beginning of the summer of 2004, when the PsNet monthly anomalies were positive, reaching values over than +0.02 kg C/m^2/month between June and September (Figure 4.10, left panel). Also, both 2004 and 2005 years had accumulated values of PsNet (0.975 and 0.967 kg C/m^2/month, respectively) above the historical median, indicating a regeneration of vegetation from 2003 drought event.

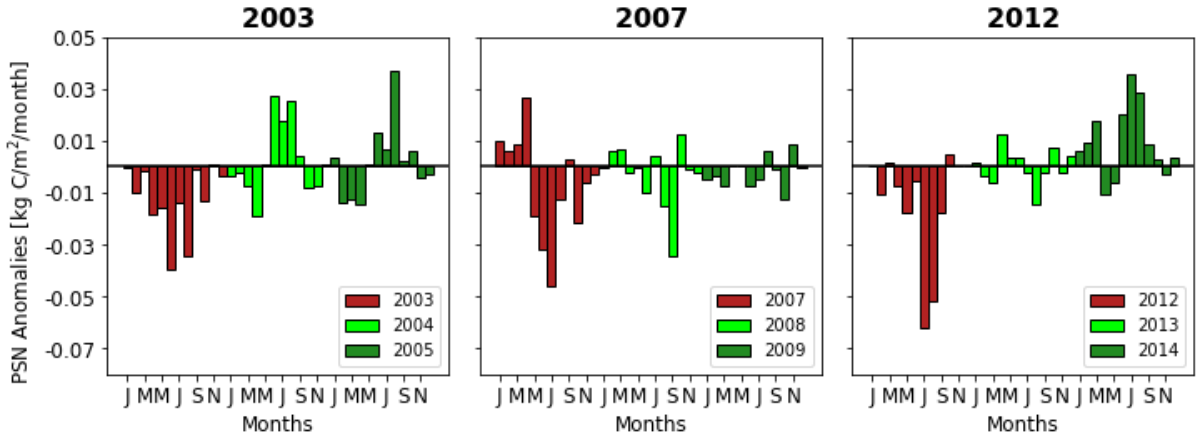

Figure 4.10 – As in Figure 4.8, but respecting to IG region for 2003 (left panel), 2007 (central panel) and 2012 (right panel).

The IG annual net photosynthesis balance during 2003, presented on Table 4.2, are, as expected, clearly negative, with losses of ~22 TgC on the region. Despite the regeneration on 2004 (+4.33 TgC) and 2005 (+3.24 TgC), the ecosystems were not able to completely recover from the 2003 drought episode.

Table 4.2 – As in Table 4.1, but respecting to IG droughts for 2003, 2007 and 2012. The monthly values are described on TgC/month and the yearly balance is described on TgC/year.

NET PHOTOSYNTHESIS LOSSES IG – 2003, 2007 AND 2012 DROUGHTS

	J	F	M	A	M	J	J	A	S	O	N	D	**TOTAL**
2003	-0.04	-1.42	-0.21	-2.65	-2.33	-5.75	-2.02	-4.94	-0.16	-1.91	0.13	-0.50	**-21.80**
2004	-0.48	-0.28	-1.04	-2.72	0.20	3.95	2.60	3.64	0.58	-1.12	-1.09	0.09	**4.33**
2005	0.48	-2.02	-1.76	-2.10	0.17	1.94	0.99	5.31	0.35	0.92	-0.57	-0.47	**3.24**
2007	1.51	0.90	1.30	4.06	-2.93	-4.95	-7.04	-1.94	0.42	-3.31	-0.97	-0.50	**-13.47**
2008	-0.06	0.91	1.00	-0.41	-0.06	-1.57	0.60	-2.36	-5.25	1.95	-0.20	-0.37	**-5.80**
2009	-0.73	-0.61	-1.16	-0.01	0.07	-1.14	-0.79	0.95	-0.14	-1.86	1.34	-0.02	**-4.10**
2012	0.02	-1.37	0.23	-0.92	-2.24	-0.71	-8.07	-6.67	-2.33	0.63	0.05	0.06	**-21.32**
2013	0.20	-0.45	-0.80	1.64	0.46	0.51	-0.33	-1.84	-0.31	0.93	-0.30	0.54	**0.25**
2014	0.79	1.19	2.27	-1.35	-0.73	2.60	4.69	3.71	1.16	0.33	-0.33	0.49	**14.80**

Concerning to the drought event of 2007 (Figure 4.9, central panel), the PsNet accumulated values over the drought affected pixels (red line) are again below the historical median of the pixels affected by drought (0.826 vs. 0.913 kg C/m^2/month). During the winter and early spring, there is an obvious higher than usual accumulation, compared with median values (Figure 4.9, central panel), as well as strong PsNet monthly anomalies between January and April (Figure 4.10, central panel). However, the negative disturbances on vegetation's photosynthesis started on May and persisted during summer, especially in June and July, when PsNet monthly anomalies reached -0.032 and -0.046 kg C/m^2/month, respectively.

Gouveia et al., (2016) analysed the catastrophic fire season in the Peloponnese Peninsula and showed that it was triggered by a possible conjunction of a severe drought in early spring, with three strong summer heatwaves. Therefore, it should be noted that, although the results in Figure 4.9 and 4.10 (central panels) correspond to the pixels affected by drought (using the methodology of the present work) within the area selected here, that includes the entire territories of Greece, Balkans and Italy. Hence, the occurrence of several months with PsNet negative anomalies throughout the IG region are probably mainly related with the three major heatwaves occurence between June and August over Greece (Tolika et al., 2009). Furthermore, the strong positive PsNet anomalies during winter and spring, which were triggered by the high occurrence of precipitation values during the fall of 2006 (Gouveia et al., 2016) and close to usual SM values in February and March (Figure 4.4), can be an indicator of high biomass availability, which combined with the high deficit of SM observed since the spring until the end of summer, increased the potential risk of large fires occurrence in summer. Moreover, even though the short drought during spring has not caused severe disturbances on IG vegetation, this event should not be underestimated because it can possibly be the takeoff of ecosystems disturbances, which were increased by the major heatwaves, and consequent large fires.

The two following years after the 2007 episode revealed values of accumulated PsNet (Figure 4.9, central panel) below the historical median (0.876 kg C/m^2/month in 2008 and 0.887 kg C/m^2/month in 2009), which indicates that the recovery process from 2007 extreme events did not occur during this period. In fact, the disturbances induced on terrestrial ecosystems can be considered the reason why vegetation got inhibited to develop a recovery process.

The 2007 annual losses on net productivity were -13.47 TgC/year and are coherent with the high accumulations of PsNet during spring and the disturbances on summer, strongly associated with the major heatwaves and consequent large fires. However, the vegetation got inhibited to recover in the following months, as the yearly balances of 2008 and 2009 remained negative, with -5.80 TgC/year and -4.10 TgC/year, respectively (Table 4.2), indicating that the 3-year period comprised between 2007 and 2009 represented a loss on IG vegetation productivity of 23.37 TgC.

The PsNet accumulated values over the drought affected pixels during the year of 2012 show huge deficits compared with the historical median (0.744 vs. 0.905 kg C/m^2/month) (Figure 4.9, right panel). Moreover, the monthly anomalies remained intensely negative during 6 consequent months, especially the extremely hazardous months of July and August, with mean anomalies of -0.062 and -0.052 kg C/m^2/month, respectively (Figure 4.10, right panel).

The PsNet results agree with GPP analysis on section 4.1.2 and can explain the severity of the impacts of drought events on ecosystems. The SM anomalies recorded on IG (Figure 4.4) showed some contrast with the anomalies recorded on PsNet during this event, with the period between January and April being quite dry, but the spring months being considered relatively wet. Therefore, this pattern is similar to the 2012 IB drought, where the vegetation could not adapt from the dry situation, which was not attenuated by the water availability during some weeks on spring.

The recovery process was weak during 2013, with 2013 PsNet accumulations (light green line) close to the historical median (0.906 kg C/m^2/month) but, during 2014 (dark green line), the vegetation recovered vigorously, presenting accumulations higher than median (0.987 vs. 0.905 kg C/m^2/month) (Figure 4.9, right panel) and, between June and September, positive mean anomalies higher than +0.01 kg C/m^2 (Figure 4.10, right panel).

The impact of 2012 drought on IG annual net photosynthesis were -21.32 TgC/year (Table 4.2). During this year, the months of June and July contributed to the vegetation productivity losses with ~15 TgC, which represents 70% of the total yearly balance. The ecosystem response to 2012 event, as mentioned before, started, weakly, during 2013 and increased, vigorously, in 2014, when the yearly balance was +14.80 TgC.

4.2.3. France Drought Event

The PsNet accumulated values of vegetation affected by the FR drought during the year of 2006 (red line) are quite significant when compared to the historical median (blue dashed line), presenting values of 0.789 vs. 0.938 kg C/m^2/month (Figure 4.11, left panel). The disturbances started on late winter and intensified along the spring months. These results are supported by observing the increasing negative values of PsNet monthly mean anomaly along the months (Figure 4.11, right panel).

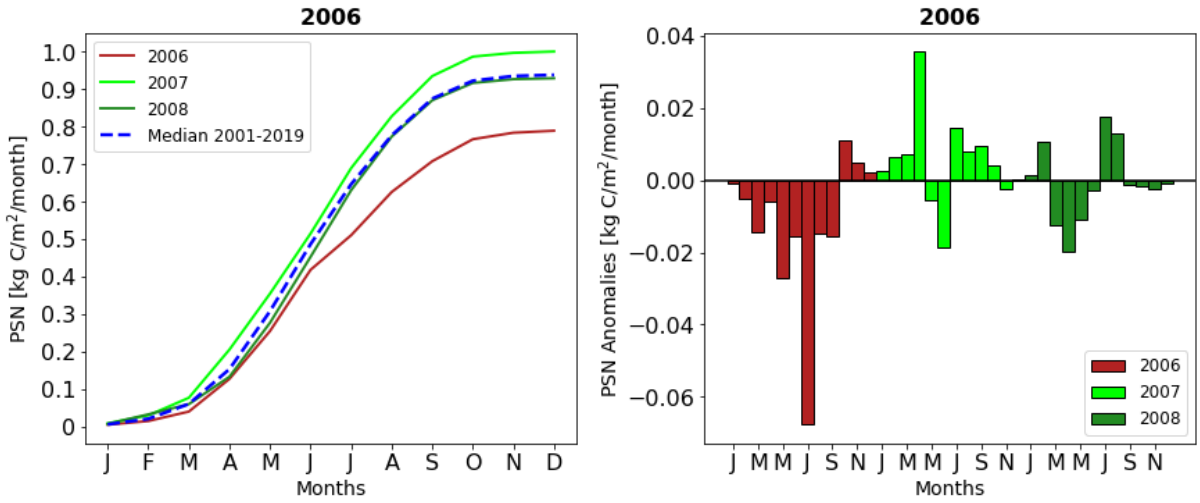

Figure 4.11 – Accumulated PsNet for the affected pixels on FR during 2006 drought (red) and the two following years of recovery (light and dark green). The accumulated historical median 2001-2019 of drought affected pixels is depicted by the blue dashed line (left panel); Averaged PsNet monthly anomaly values over selected pixels during the drought year (red) and the following two years (light and dark green) for the drought episode of 2006 (right panel.

The SM results demonstrate the presence of dry conditions since late winter/beginning of spring, despite the water availability during some weeks on spring (Figure 4.4). Moreover, a strong heatwave on July (Rebetez et al., 2009) seems to enhance the consequences on vegetation productivity of the region, especially on summer, with an intense negative anomaly during July (-0.068 kg C/m^2) (Figure 4.11, right panel). Under these conditions, the PsNet information agree with the GPP results, explaining the reason why several areas of FR were 3-4 months below the regional threshold.

The recovery from 2006 drought seems to occur during 2007, with accumulations of PsNet (light green line) higher than historical median (1.00 kg C/m^2/month) (Figure 4.11, left panel) and a positive yearly balance of vegetation productivity of +11.12 TgC /year (Table 4.3). However, this is only about 42% of recovery from the -26.52 TgC/year losses that occurred due to the 2006 extreme event. Therefore, and since 2008 had practically null productivity balance, the FR vegetation affected by the 2006 drought did not entirely recover.

Table 4.3 - As in Table 4.1 but respecting to FR drought for 2006. The monthly values are described on TgC/month and the yearly balance is described on TgC/year.

NET PHOTOSYNTHESIS LOSSES FR - 2006 DROUGHT

	J	F	M	A	M	J	J	A	S	O	N	D	**TOTAL**
2006	-0.16	-0.89	-2.56	-0.96	-4.72	-2.88	-12.14	-2.61	-2.83	1.96	0.87	0.40	**-26.52**
2007	0.47	1.18	1.29	6.31	-0.98	-3.26	2.62	1.44	1.69	0.74	-0.43	0.05	**11.12**
2008	0.24	1.90	-2.21	-3.47	-2.00	-0.54	3.22	2.32	-0.16	-0.28	-0.45	-0.13	**-1.58**

4.3. Impact of Fires on Vegetation Net Photosynthesis

4.3.1. Iberian Peninsula Large Fires

The IB burned areas of 2003, 2005, 2012 and 2017, obtained from FireCCI51 product, are represented on Figure 4.12, where the red points represent the burned areas for each fire season and were selected from the Julian Day (JD) dataset.

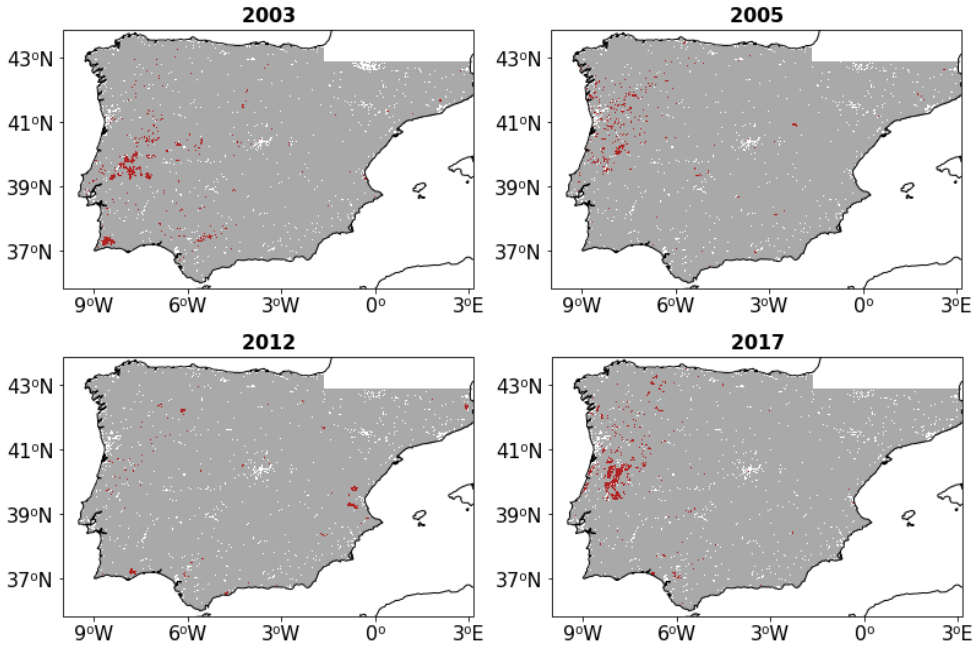

Figure 4.12 – BAs on IB during 2003 (upper left panel), 2005 (upper right panel), 2012 (bottom left panel) and 2017 (bottom right panel).

The BAs are the result of a sensibility analysis (Figures 4.13 and A.2), by using the Confidence Level (CL) dataset from FireCCI51 for each considered year. Most of the burned pixels selected on JD dataset have a confidence level above 90%, with some points varying between 70-90% of confidence, indicating that the dataset is quite robust (Figure 4.13, left panel). This process was made for all the years considered and study regions (Table 3.2) (Figures A.2, A.3 and A.4).

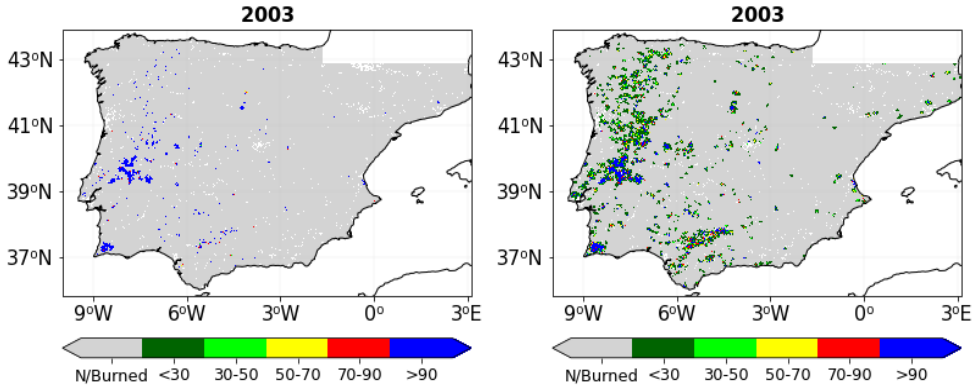

Figure 4.13 – Level of confidence of detected burned pixels (left panel) and of all the detected pixels incorporated on CL dataset (right panel) for 2003 fire season over IB.

The fire seasons of 2003 and 2017 in Portugal were particularly catastrophic, especially the central region of the country (Figure 4.12, left top panel and right bottom panel, respectively) (Trigo et al., 2006; Turco et al., 2019). For both years, the values of accumulated PsNet (red line) are below the historical median over the selected burned pixels (blue dashed line), respectively 0.805 vs. 0.859 kg C/m^2/month and 0.861 vs. 0.944 kg C/m^2/month (Figure 4.14, left top and right bottom panels). However, the deficit of values compared to the median is low, considering the extension of BAs. This low deficit can be explained due to the PsNet accumulation values higher than historical median occurred in the first half the year, especially during spring. Thus, there was a high biomass accumulation, due to higher than normal photosynthetic activity, leading to large fires which may be linked to the impact of major heatwaves (EMDAT, Trigo et al., 2006). The high vegetation's dynamics can be also observed in Figure 4.15, with monthly mean PsNet anomalies being positive between May and July of 2003 (Figure 4.15, left top panel) and between January and April of 2017 (Figure 4.15, right bottom panel). Therefore, despite the intensity of fires and the extension of BAs, the accumulations during these years were not lower due to the compensation of positive PsNet anomalies during late winter and spring seasons.

The impacts on vegetation productivity are described on Table 4.4. The final balance is -0.51 TgC/year in 2003, with the months of August and September representing ~ 67% of yearly net productivity disturbances, and -0.93 TgC/year in 2017, mainly associated to the large fire of Pedrógão Grande-Góis in June (Pinto et al., 2018) that represents 37% of productivity losses occurred between June and December, and large fires in October associated to the dry conditions of soil and stress of vegetation, high temperatures (Turco et al., 2019) and, also to the hurricane Ophelia, indicating not only the severity of fires, but also, the intensity and incidence of these events on ecosystems (ICNF report 2017).

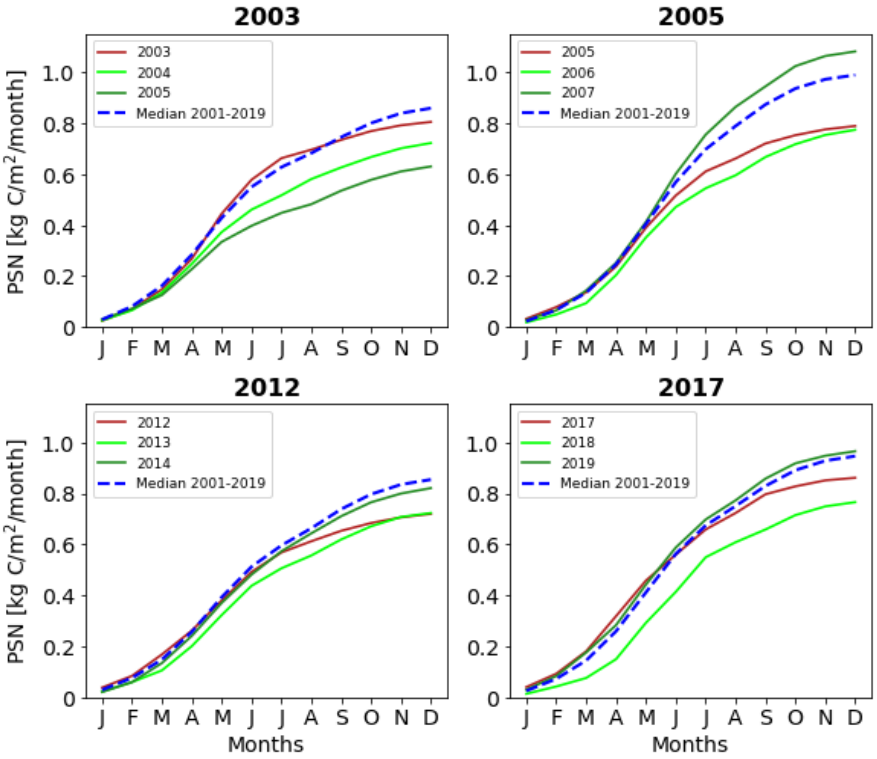

Figure 4.14 - Accumulated PsNet on IB for the considered affected pixels during the year of large fires (red) and the two following years of recovery (light and dark green) for 2003 (upper left panel), 2005 (upper right panel), 2012 (bottom left panel) and 2017 (bottom right panel). The accumulated historical median 2001-2019 of drought affected pixels is depicted by the blue dashed line.

In spite of some similarity within the conditions present both in 2003 and 2017, the vegetation response on these two years was completely different. On one hand, there was no recovery, at all, in the two following years after the 2003 fire events (Figures 4.14 and 4.15, left top panels). In fact, the disturbances on ecosystems increased in 2004 (light green line), and especially in 2005 (dark green line), when the accumulated PsNet was even lower than 2003 (0.722 kg C/m^2/month and 0.630 kg C/m^2/month, respectively), mainly associated to the outstanding drought stated previously (García-Herrera et al., 2007, Gouveia et al., 2009, 2012). The drought episode contributed to the increasing losses on productivity, with negative yearly productivity balances in 2004 and 2005 (-1.00 TgC/year and -1.67 TgC/year, respectively) (Table 4.4). Therefore, the burned pixels during this 3-year period (2003-2005) contributed with -3.18 TgC to the IB vegetation productivity balance.

One the other hand, the vegetation burned on 2017 fires presented a slight recovery in 2019 (Figures 4.14 and 4.15, right bottom panels). Nevertheless, until then, the response to the extreme fires did not occur, and this is very well depicted on PsNet results (Figures 4.17d and 4.18d). The disturbances induced on vegetation's dynamics by large fires were so severe that, although the meteorological conditions were favourable to vegetation regeneration during 2018, with water availability on soil and temperatures lower than mean (Buras et al., 2020) during several months, the IB affected ecosystems were not able recover. In fact, the 2018 yearly productivity balance was -1.28 TgC/year, with the first half of the year representing 83% of the productivity losses. Hence, the burned areas of 2017 fire season had a contribution, during the period 2017-2019, of -2.06 TgC to the net photosynthesis balance.

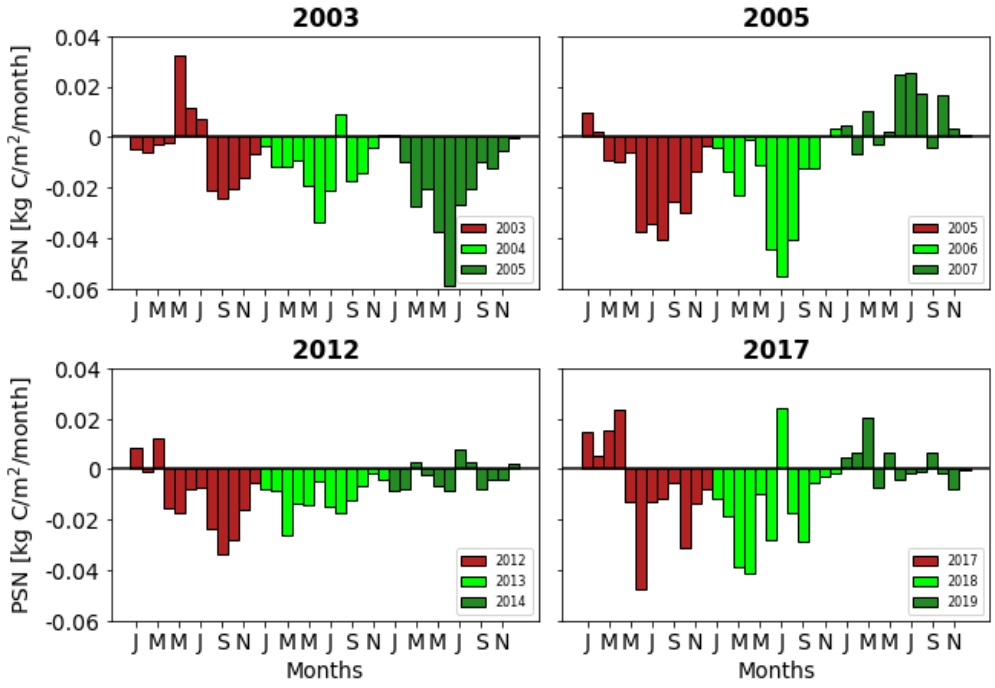

Figure 4.15 - Averaged PsNet monthly anomaly values over selected pixels during the drought year (red) and the following two years (light and dark green) for the large fires of 2003 (upper left panel), 2005 (upper right panel), 2012 (bottom left panel) and 2017 (bottom right panel) over IB region.

The large fires of 2005 on IB affected particularly the northern region of Portugal (Figure 4.12, right top panel). The 2005 PsNet accumulated values (red line) over burned pixels were strongly below the historical median of 2005 burned pixels (0.789 vs. 0.988 kg C/m^2/month) (blue dashed line). As stated in previous sections, during 2005, the IB was severely influenced by a strong drought. Therefore, the dry conditions, both of soil and vegetation, may had been the trigger of the large fires. In fact, the

PsNet monthly mean anomalies reached values lower than -0.03 kg C/m^2/month (Figure 4.14, right top panel), and the productivity losses between June and December reached -1.01 TgC/year, which clearly depicts the influence of drought, and consequent large fires, simultaneously, on vegetation's activity.

Again, for the 2012 case study, the accumulated values of PsNet (red line) were far below the historical median (blue dashed line) of burned pixels (0.720 vs. 0.854 kg C/m^2/month). Although the total BA is smaller than the other analysed years previously, IB region was under drought influence during 2012, indicating that the negative anomalies of PsNet (Figure 4.15, left bottom panel) during summer season may be explained by the drought event, and its associated fires.

In terms of terrestrial ecosystem response, the years of 2005 and 2012 have a similar behaviour, as the recovery only occurred two years later. In 2005, after the intense drought, the vegetation did not recover in 2006 due to the summer heatwave. The PsNet mean anomalies reached values around -0.05 kg C/m^2/month and the losses on plants productivity during this year were -1.16 TgC/year, which is higher than 2005 losses due to the possible combined effect of burned vegetation, summer heatwave and drought effects (Figure 4.15, left bottom panel, Table 4.4). Afterwards, in 2007, the photosynthesis rates showed a strong recovery, especially in summer (Figures 4.14 and 4.15, left bottom panels). Nevertheless, the positive balance during 2007 does not offset the losses occurred in 2005 and 2006, and the 3-year period net productivity balance (2005-2007) is -1.67 TgC. In the case of 2012, the vegetation had a weak process of regeneration, showing accumulated values of PsNet during 2013 (light green line) close to 2012's case and, in the end of the year of 2014 (dark green line), the affected burned pixels accumulated 0.821 kg C/m^2/month, which is close to the historical median value (0.854 kg C/m^2/month). The results of the yearly net photosynthesis balance (Table 4.4) are reinforced by the 2013 productivity losses which were higher than in 2012 (-0.30 TgC/year) and was practically null during 2014 (-0.08 TgC/year), therefore indicating the weak response.

Table 4.4 - Quantification of net photosynthesis disturbances, with monthly and yearly balances for 2003, 2005, 2012 and 2017 IB large fires. The monthly values are described on TgC/month and the yearly balance is described on TgC/year.

NET PHOTOSYNTHESIS LOSSES IB – 2003, 2005, 2012 AND 2017 BURNED AREAS

	J	F	M	A	M	J	J	A	S	O	N	D	**TOTAL**
2003	-	-	-	-	-	0.08	0.05	-0.16	-0.18	-0.15	-0.12	-0.05	**-0.51**
2004	-0.02	-0.09	-0.08	-0.07	-0.14	-0.25	-0.16	0.06	-0.13	-0.10	-0.03	0.01	**-1.00**
2005	0.01	-0.07	-0.20	-0.15	-0.27	-0.43	-0.20	-0.15	-0.07	-0.09	-0.04	-0.00	**-1.67**
2005	-	-	-	-	-	-0.21	-0.19	-0.22	-0.14	-0.16	-0.07	-0.02	**-1.01**
2006	-0.02	-0.07	-0.13	-0.01	-0.06	-0.24	-0.30	-0.22	-0.07	-0.07	0.00	0.02	**-1.16**
2007	0.03	-0.03	0.06	-0.02	0.01	0.14	0.14	0.09	-0.02	0.09	0.02	0.01	**0.50**
2012	-	-	-	-	-	-0.02	-0.02	-0.06	-0.08	-0.07	-0.04	-0.01	**-0.28**
2013	-0.02	-0.02	-0.06	-0.03	-0.03	-0.01	-0.03	-0.04	-0.03	-0.02	-0.00	-0.01	**-0.30**
2014	-0.02	-0.02	0.01	-0.01	-0.02	-0.02	0.02	0.01	-0.02	-0.01	-0.01	0.00	**-0.08**
2017	-	-	-	-	-	-0.34	-0.09	-0.08	-0.04	-0.22	-0.10	-0.06	**-0.93**
2018	-0.09	-0.13	-0.28	-0.29	-0.07	-0.20	0.18	-0.12	-0.21	-0.04	-0.02	-0.01	**-1.28**
2019	0.03	0.05	0.14	-0.05	0.04	-0.03	-0.01	-0.01	0.05	-0.01	-0.05	-0.00	**0.15**

4.3.2. Italia and Greece Large Fires

The largest fires in IG occurred in 2007, namely over Greece (Figure 4.16, left panel), which led to intense perturbations on local vegetation (Gouveia et al., 2016), and, in several territories on Italy and Balkans during 2012 (Figure 4.16, central panel). In 2017, there were also some BAs in Balkans and Carpathian regions and some burned spots in Sicily, Italy (Figure 4.16, right panel).

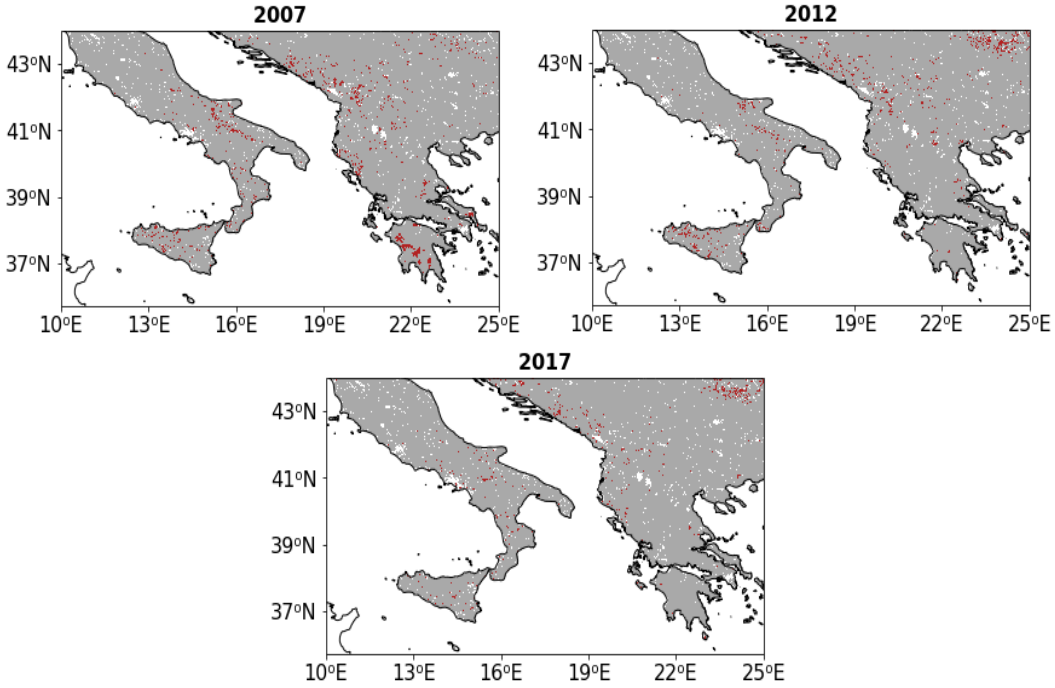

Figure 4.16 – As in Figure 4.12, but respecting to IG region for 2007 (upper left panel), 2012 (upper right panel) and 2017 (bottom central panel).

The burned area in IG region reached a total extension of 11 726 km^2 in 2007, representing 2.72% of the total area of territory (Table 3.3). The fires affected large areas of Greece, namely Peloponnese Peninsula, burning 223 724 ha, which was the highest BA ever recorded on the country. These intense fires led to severe disturbances on vegetation (Koutsias et al., 2012; Gouveia et al., 2016). The values of PsNet accumulated (Figure 4.17, left panel) during 2007 (red line) are below the historical median (blue dashed line) of burned 2007 area pixels (0.773 vs. 0.854 kg C/m^2/month). The results show a strong activity of vegetation during the January-April period (Figures 4.16 and 4.17, left panel), which may be associated to the availability of biomass, easily burned on the presence of a triggering extreme event, such as the exceptional heatwaves that occurred from June to August, or the drought conditions in the end of spring. This pattern of high accumulation values of PsNet during winter or spring and the large fires during summer associated to extreme climatic events which has the capability to become exacerbated due to the high availability of biomass, is quite similar to the episodes occurred in 2003 and 2017 on IB. Naturally, these combined situations induced losses on vegetation productivity between June and December of -1.39 TgC/year, representing the months of June and July, together, 43% of the yearly productivity disturbances (Table 4.5).

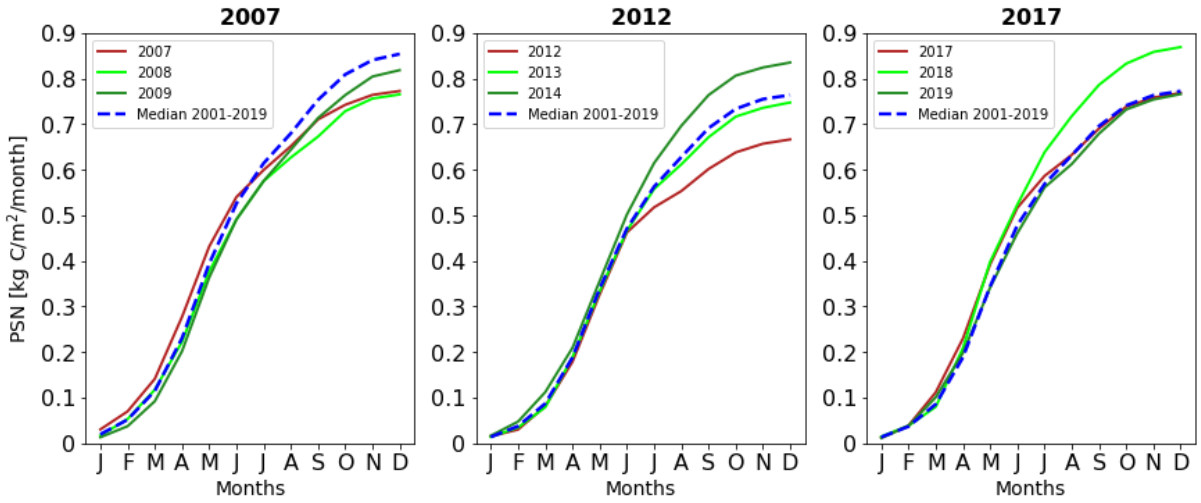

Figure 4.17 - As in Figure 4.14, but respecting to IG region for 2007 (left panel), 2012 (central panel) and 2017 (right panel).

The large fires associated to extreme events occurred in 2007 led to slowly recovery of vegetation, as the two following years did not show a clear regeneration response. The accumulated PsNet values are below the historical median, and the monthly anomalies remained negative for several consecutive months in 2008 and 2009 (Figures 4.17 and 4.18, left panels). Also, the productivity yearly balance for 2008 and 2009 (Table 4.5) is clearly negative (-1.05 TgC/year in 2008 and -0.49 TgC/year in 2009). These results indicate that the vegetation was disturbed after the 2007 large fires, highlighting the severity of the events. Therefore, the burned vegetation had, in this 3-year period (2007-2009) contributed with -2.86 TgC to the IG productivity losses.

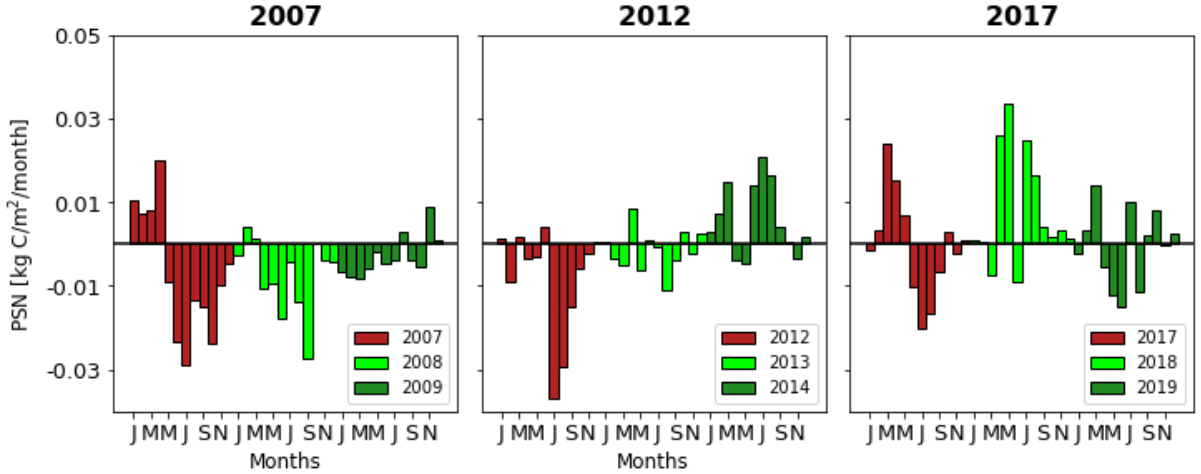

Figure 4.18 – As in Figure 4.15, but respecting to IG region for 2007 (left panel), 2012 (central panel) and 2017 (right panel).

The spatial pattern of BAs during 2012 (Figure 4.16, central panel) pointed out the dramatic fire season on Sicily and some areas on the Balkans. Naturally, these regions had a great contribution to the deficit on PsNet during 2012. The low PsNet accumulation over the burned pixels (0.666 vs. 0.764 kg C/m^2/month), as well as the consecutive negative monthly mean anomalies during summer (Figures 4.17 and 4.18, central panels, respectively) are a clear evidence of the hazardous character of the fire season

over the region. Consequently, there were strong impacts on net photosynthesis balance, with disturbances of -0.76 TgC/year, between June and December of 2012 (Table 4.5). The vegetation showed a slightly regeneration in 2013, with an annual balance of -0.15 TgC/year, with alternate positive and negative monthly balances during the year. In 2014, the vegetation seems to be almost recovered from 2012 events, by presenting a positive annual productivity of +0.64 TgC/year.

The patterns of 2012 large fires impact's on IG seems to have some similarity to the IB 2005 and 2012 cases, mainly due to the triggering climatic element of fires (critical drought situation). Furthermore, the ecosystems recovery occurs several months after the extreme event.

The burned area during the fire season of 2017 on IG region was 6 738 km^2, and most of the BA is localized on the Balkans and the Carpathian Mountains (Figure 4.16, right panel). The situation is similar to 2007 spring, with high monthly accumulated PsNet values (Figure 4.17, right panel), which can translate into a healthy vegetation with high production rates. However, unlike 2007, the 2017 summer in IG seems to have less intense and frequent extreme climatic events, which prevented the strong propagation of large fires in the region, despite the healthiness of vegetation and the high availability of biomass in the ecosystems. Nevertheless, the fires occurred in summer led to losses on productivity of about 0.35 TgC/year, with the highest value being observed in July (Table 4.5).

The recovery process in 2018 was quite intense, with accumulations of PsNet (light green line on Figure 4.18, right panel) higher than historical median (0.869 vs. 0.772 kg C/m^2/month), indicating a strong response of the vegetation burned in the previous year. Naturally, the positive response is translated into a positive yearly balance of +0.64 TgC, which offset all the losses occurred due to the large fires of 2017.

Table 4.5 - As in Table 4.4 but respecting to IG large fires for 2007, 2012 and 2017. The monthly values are described on TgC/month and the yearly balance is described on TgC/year.

NET PHOTOSYNTHESIS LOSSES IG – 2007, 2012 AND 2017 BURNED AREAS

	J	F	M	A	M	J	J	A	S	O	N	D	**TOTAL**
2007	-	-	-	-	-	-0.27	-0.33	-0.15	-0.18	-0.28	-0.12	-0.06	**-1.39**
2008	-0.03	0.05	0.01	-0.13	-0.11	-0.28	-0.05	-0.16	-0.32	-0.00	-0.05	-0.05	**-1.05**
2009	-0.08	-0.09	-0.10	-0.07	-0.02	-0.05	-0.05	0.03	-0.05	-0.06	0.11	0.01	**-0.42**
2012	-	-	-	-	-	0.03	-0.33	-0.26	-0.13	-0.05	-0.02	0.00	**-0.76**
2013	0.00	-0.03	-0.04	0.08	-0.06	0.01	-0.00	-0.10	-0.03	0.03	-0.02	0.02	**-0.15**
2014	0.03	0.07	0.13	-0.03	-0.04	0.13	0.19	0.15	0.04	0.00	-0.03	0.02	**0.64**
2017	-	-	-	-	-	-0.07	-0.14	-0.11	-0.04	0.02	-0.02	0.01	**-0.35**
2018	0.01	0.00	-0.05	0.17	0.22	-0.06	0.16	0.11	0.03	0.01	0.02	0.01	**0.64**
2019	-0.01	0.02	0.09	-0.04	-0.08	-0.10	0.07	-0.08	0.02	0.05	-0.00	0.02	**-0.04**

4.3.3. France Large Fires

Two years were chosen as study cases for the FR region, namely 2003 and 2017. In comparison with the two prior study regions, IB and IG, the BA in the FR is, by far, smaller, causing less damage on local vegetation and on terrestrial carbon uptake. However, despite these considerations, both years had BAs higher than the FR average 1980-2019 (Table 3.2), and induced disturbances on productivity levels.

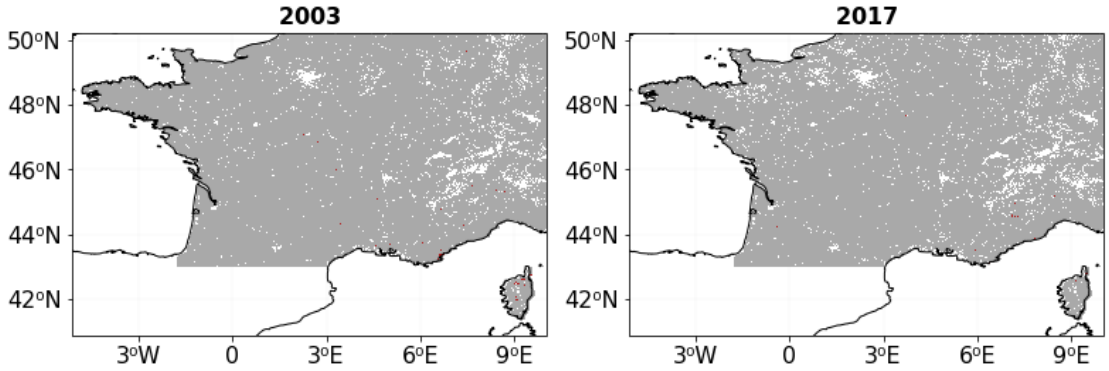

Figure 4.19 – As in Figure 4.12, but respecting to FR region during 2003 (left panel) and 2017 (right panel).

The burned areas occurred in the South of France and, especially, on Corsica during 2003 (Figure 4.19, left panel). During this year, the accumulation of PsNet (red line) were significantly low, compared with the historical median (dashed blue line) over the burned pixels in 2003, being 0.790 vs. 0.981 kg C/m^2/month (Figure 4.20, left panel). The disturbances had their takeoff in July, which corresponds to the month when one of the strongest heatwaves struck Southwestern Europe (EMDAT, Trigo et al., 2005; Bastos et al., 2014), that might be associated with the large fires of 2003 in the region. The Figure 4.21 (left panel) highlights the possible impacts on photosynthetic activity, with PsNet monthly anomaly reaching -0.062 kg C/m^2/month in July. The negative anomalies lasted in the next consecutively months, until the middle of 2004. Therefore, the large fires, associated with the summer heatwave, induced a negative annual balance of net productivity, between June and December of 2003, of -0.17 TgC/year.

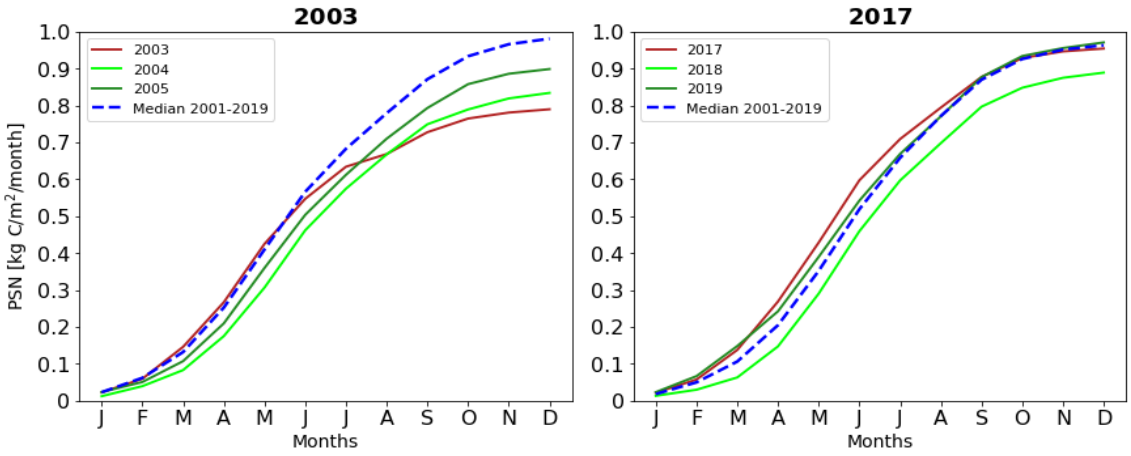

Figure 4.20 - As in Figure 4.13, but respecting to FR region for 2003 (left panel) and 2017 (right panel).

The vegetation recovery did not occur in 2004 and 2005 (Figures 4.20 and 4.21, left panels). During 2004, the accumulated value of PsNet (light green line) was 0.834 kg C/m^2/month and in 2005 was 0.899 kg C/m^2/month. Consequently, the annual net photosynthesis balance was negative on both years (-0.12 TgC/year and -0.07 TgC/year, respectively). Therefore, despite the extension of BA was low, compared with the other study regions, the FR large fires in 2003, were severe, and left scars on local vegetation.

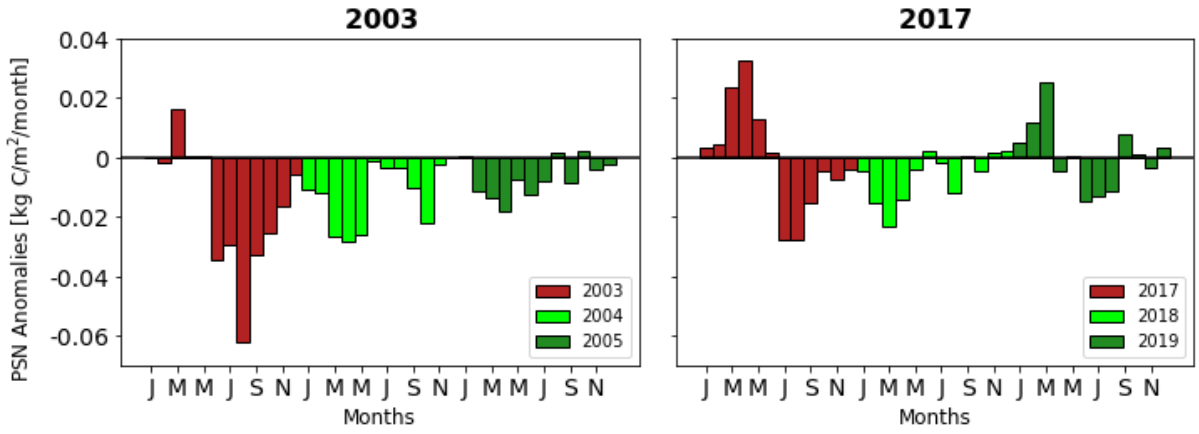

Figure 4.21 – As in Figure 4.14, but respecting to FR region for 2003 (left panel) and 2017 (right panel).

In 2017, the BAs were scattered throughout the South of France (Figure 4.19, right panel). Despite the fires occurence, the effects can be offset due to the high greenness of the vegetation until June/July, because, before these months, the accumulated values were higher than the historical median and the monthly anomalies of PsNet were positive (Figures 4.20 and 4.21, right panels).

On the other side, the disturbances are still visible in 2018, as obtained by the accumulated PsNet (light green line) that is considerably below the historical median (0.889 kg C/m^2/month) (Figure 4.20, right panel). Therefore, the regeneration of vegetation, after the 2017 fires on FR did not occurred in 2018 nor in 2019, with the yearly balance revealing productivity losses of -0.02 TgC/year, both in 2017 and 2018, and being neutral on 2019.

Table 4.6 – As in Table 4.4 but respecting to FR large fires for 2003 and 2017. The monthly values are described on TgC/month and the yearly balance is described on TgC/year.

NET PHOTOSYNTHESIS LOSSES FR – 2003 AND 2017 BURNED AREAS

	J	F	M	A	M	J	J	A	S	O	N	D	**TOTAL**
2003	-	-	-	-	-	-0.03	-0.02	-0.05	-0.03	-0.02	-0.01	-0.00	**-0.17**
2004	-0.01	-0.01	-0.02	-0.02	-0.02	-0.00	-0.00	-0.00	-0.01	-0.02	-0.00	-0.00	**-0.12**
2005	0.00	-0.01	-0.01	-0.01	-0.01	-0.01	-0.01	0.00	-0.01	0.00	-0.00	-0.00	**-0.07**
2017	-	-	-	-	-	0.00	-0.01	-0.01	-0.00	-0.00	-0.00	-0.00	**-0.02**
2018	-0.00	-0.00	-0.01	-0.00	-0.00	0.00	-0.00	-0.00	0.00	-0.00	0.00	0.00	**-0.02**
2019	0.00	0.00	0.01	-0.00	0.00	-0.00	-0.00	-0.00	0.00	0.00	-0.00	0.00	**0.00**

5. Conclusions

This study proposes to analyze how droughts and large fires disturb the Mediterranean vegetation gross productivity and net photosynthesis, by observing a set of severe episodes of both extremes, between 2001 and 2019, and quantifying the productivity losses and disturbances of vegetation activity. The analysis is based on remote sense products, namely GPP, PsNet, SM and FireCCI, guaranteeing an appropriate monitorization of vegetation and the influence of climatic extreme events, and associated large fires, in terrestrial ecosystems. Furthermore, this work intends to assess the ecosystems regeneration after extreme episodes, by analyzing the following two years after each event.

The statistical characterization of SM anomaly fields, combined with the methodology used to detect droughts, based on the definition of one anomaly threshold of GPP for each region, allowed the observation of the persistence of dry conditions over the vegetation throughout the different study areas. Moreover, the methodologies applied to PsNet fields, to determine the disturbances of each extreme episode, enabled the quantification of vegetation productivity losses caused by the most hazardous drought episodes and large fires occurred during the study period. This analysis was made separately for droughts and fires, and for each one of the study areas, identifying widespread negative PsNet anomalies during the most extreme events in all regions, associated to patterns of large deficits on soil moisture and large fires, respectively. Nevertheless, the most extreme years are not the same for the different study areas, namely in the case of droughts:

- Over IB, both drought events of 2005 and 2012 caused large deficits on soil moisture, especially during late winter and spring seasons, which strongly contributed to exacerbate the losses on plants productivity. However, the drought event of 2005 covered a larger extension in terms of the impacts on ecosystems (250 712 km^2 against 147 217 km^2 in 2012) with the vegetation remaining under persistent dry conditions during a longer period. The results are in line with the works of García-Herrera et al., (2007) and Gouveia et al., (2009, 2012) that pointed out the outstanding characteristics of the 2004-2005 drought, which had several consequences on IB plants activity. The scars left on ecosystems activity were clearly depicted on the huge negative annual balance of net productivity during 2005 (~ -40 TgC/year), which inhibited the vegetation to recover in the following months.
- Similarly, drought events severely disturbed the ecosystems of the Italian Peninsula in 2003, Greece in 2007 and the Balkans in 2012. These climatic events were characterized by accentuated deficits of soil moisture. During 2003 and 2012, not only the photosynthetic activity was strongly affected by the drought, showing low accumulated values during the year, and also large productivity losses. The consequences of droughts in both years extended over several months, as the vegetation showed weak and slow recovery in the two years after the extreme events. During 2007, the terrestrial ecosystems of IG were affected by a drought during spring and, also, by three major heatwaves in the summer, which triggered large fires, especially in Greece (Tolika et al., 2009). The occurrence of a compound event (Gouveia et al., 2016) exacerbated the disturbances on plants activity during 2007, but either in 2008 and 2009, as the vegetation was inhibited to recover, showing low photosynthetic activity and negative annual net photosynthesis balance in both years.
- Over FR region, the influence of 2006 drought event on ecosystems spread throughout the territory, with 3 to 4 months of dry conditions, severely disturbing the vegetation productivity. Nevertheless, the terrestrial ecosystems showed a regeneration from the event during 2007 and 2008.

On the other hand, in the case of fires:

- In the Iberian Peninsula, the fire seasons of 2003 and 2017 were particularly catastrophic (Trigo et al., 2006), mainly due to two important triggering elements: the higher than usual activity of vegeta-

tion during late winter and spring seasons, which indicated the availability of biomass, and the occurrence of an extreme heatwave, during summer. The conjunction of these two elements led to intense fires that induced severe consequences on productivity and inhibited the vegetation to recover in the following months. In the case of 2005 and 2012, the large fires were triggered mainly due to the critical dry conditions, which led to a highly decrease on the vegetation's productivity rates.

- Concerning to the IG region, the 2007 fire season was catastrophic, especially in Greece (Gouveia et al., 2016). The exceptional summer heatwaves and the drought established during late spring, in conjunction with the high availability of biomass, led to the occurrence of large fires and inhibited the vegetation to regenerate in the following months. Moreover, the 2012 fire season, that affected mainly the Sicilian territory, was somehow similar to the IB 2005 and 2012 study cases, mainly due to the critical drought that triggered the fires, inducing a weak regeneration on affected ecosystems after the events. Conversely, during 2017, despite the intensity of fires, especially in Balkans Carpathian Mountains, the vegetation showed a strong recovery process.
- The fire seasons throughout France in 2003 and 2017 affected Corsica and the South France. The intensity and extension of FR fires, compared with the large fires of IB and IG, are lower and have a smaller influence on net photosynthesis. Nevertheless, both fire seasons left scars on local vegetation.

Therefore, the assessment of the most hazardous drought events throughout the Mediterranean region allowed to examine the remarkable influence that dry persistent conditions have on vegetation dynamics and productivity, both during the occurrence of the event and afterwards, during the regeneration period. Moreover, their conjunction with heatwaves, as described on literature regarding the IG 2007 episode, amplify the disturbances on terrestrial ecosystems, that might last from months to years, inhibiting their recovery from the extreme events and exacerbate the losses on productivity. Hence, the impact of heatwaves on vegetation activity is still an important topic to analyse, in order to conceptualize the net productivity disturbances due to the simultaneous occurrence of drought and heatwave events. Beyond that, the projected rise in temperature and droughts frequency, as well as a decrease in precipitation for the Mediterranean regions (IPCC SR1.5, 2018), may lead, in the future, to an increase of intensity and frequency of heatwaves, droughts, and also the combination of both (Zscheischler et al., 2018).

The results of disturbances on vegetation activity due to large fires allow to conclude that the most severe fire seasons are associated to the availability of biomass that easily burns in the presence of a climatic extreme event, like a summer heatwave, as occurred in IB in 2003 and 2017 or IG in 2007, or also persistent droughts, as occurred in IB in 2005 and 2012 or IG in 2012. Furthermore, these episodes generally contributed to increase the amounts of CO_2 in the atmosphere, as result of burned vegetation and forests which store carbon. Hence, it is important, as future work, to relate these extreme events with fire emissions towards atmosphere that increase the atmospheric CO_2 concentrations.

In conclusion, the analysis of these events over three different regions of Mediterranean basin, by using methods able to detect droughts, to evaluate the persistence of dry conditions and to quantify the disturbances on vegetation net productivity, clarified the consequences that these extreme events had on vegetation, either during the episode and during the recovery period. The detection of burned areas, combined with the methodologies applied to quantify the net photosynthesis losses, also allowed to assess the disturbances that large fires have, particularly, on carbon cycle, considering the net productivity deficit occurred in a short period of time, and the perturbations induced on ecosystems recovery in the following months, that amplify the productivity losses during a long period of time. Finally, it should be stressed the importance to assess the impact of simultaneous drought and large fires, or even heatwaves, in ecosystems due to the potential influence which drought events may have on the recovery response of burned vegetation.

6. References

Ballantyne, A., Smith, W., Anderegg, W., Kauppi, P., Sarmiento, J., Tans, P., Shevliakova, E., Pan, Y., Poulter, B., Anav, A., Friedlingstein, P., Houghton, R., Running, S., (2017). "Accelerating net terrestrial carbon uptake during the warming hiatus due to reduced respiration". *Nat. Clim. Chang.* 7, 148-152. https://doi.org/10.1038/nclimate3204

Barriopedro, D., Fischer, E.M., Luterbacher, J., Trigo, R.M., García-Herrera, R., (2011). "The hot summer of 2010: Redrawing the temperature record map of Europe". *Science* 332, 220-224. https://doi.org/10.1126/science.1201224

Bastos, A., Fu, Z., Ciais, P., Friedlingstein, P., Sitch, S., Pongratz, J., Weber, U., Reichstein, M., Anthoni, P., Arneth, A., Haverd, V., Jain, A., Joetzjer, E., Knauer, J., Lienert, S., Loughran, T., McGuire, P.C., Obermeier, W., Padrón, R.S., Shi, H., Tian, H., Viovy, N., Zaehle, S., (2020). "Impacts of extreme summers on European ecosystems: A comparative analysis of 2003, 2010 and 2018: European extreme summers and the C-cycle". *Philos. Trans. R. Soc. B Biol. Sci*. 375, https://doi.org/10.1098/rstb.2019.0507

Bastos, A., Gouveia, C.M., Dacamara, C.C., Trigo, R.M., (2011). "Modelling post-fire vegetation recovery in Portugal". *Biogeosciences* 8, 3593–3607. https://doi.org/10.5194/bg-8-3593-2011

Bastos, A., Gouveia, C.M., Trigo, R.M., Running, S.W., (2014). "Analysing the spatio-temporal impacts of the 2003 and 2010 extreme heatwaves on plant productivity in Europe". *Biogeosciences*. 11, 3421-3435. https://doi.org/10.5194/bg-11-3421-2014

Bolten, J.D., Crow, W.T., (2012). "Improved prediction of quasi-global vegetation conditions using remotely-sensed surface soil moisture". *Geophys. Res. Lett.* 39, L19406. https://doi.org/10.1029/2012GL053470

Buras, A., Rammig, A., Zang, C.S., (2020). "Quantifying impacts of the 2018 drought on European ecosystems in comparison to 2003". *Biogeosciences.* 17, 1655-1672. https://doi.org/10.5194/bg-17-1655-2020

Caon, L., Vallejo, V.R., Coen, R.J., Geissen, V., (2014). "Effects of wildfire on soil nutrients in Mediterranean ecosystems". *Earth-Science Rev*. 139, 47-58, https://doi.org/10.1016/j.earscirev.2014.09.001

Casagrande, E., Mueller, B., Miralles, D.G., Entekhabi, D., Molini, A., (2015). "Wavelet correlations to reveal multiscale coupling in geophysical systems". *J. Geophys. Res.* 120, 7555-7572, https://doi.org/10.1002/2015JD023265

Chuvieco, E., Lizundia-Loiola, J., Lucrecia Pettinari, M., Ramo, R., Padilla, M., Tansey, K., Mouillot, F., Laurent, P., Storm, T., Heil, A., Plummer, S., (2018). "Generation and analysis of a new global burned area product based on MODIS 250 m reflectance bands and thermal anomalies". *Earth Syst. Sci. Data*. 10, 2015–2031, https://doi.org/10.5194/essd-10-2015-2018

Ciais, P., Reichstein, M., Viovy, N., Granier, A., Ogée, J., Allard, V., Aubinet, M., Buchmann, N., Bernhofer, C., Carrara, A., Chevallier, F., De Noblet, N., Friend, A.D., Friedlingstein, P., Grünwald, T., Heinesch, B., Keronen, P., Knohl, A., Krinner, G., Loustau, D., Manca, G., Matteucci, G., Miglietta, F., Ourcival, J.M., Papale, D., Pilegaard, K., Rambal, S., Seufert, G., Soussana, J.F., Sanz, M.J., Schulze, E.D., Vesala, T., Valentini, R., (2005). "Europe-wide reduction in primary productivity caused by the heat and drought in 2003". *Nature* 437, 529-533, https://doi.org/10.1038/nature03972

Del Grosso, S., Parton, W., Stohlgren, T., Zheng, D., Bachelet, D., Prince, S., Hibbard, K., Olson, R., (2008). "Global potential net primary production predicted from vegetation class, precipitation, and temperature". *Ecology* 89(8) 2117-2126. https://doi.org/10.1890/07-0850.1

Delworth, T.L., Manabe, S., (1988). "The Influence of Potential Evaporation on the Variabilities of Simulated Soil Wetness and Climate". *J. Clim.* 5, 523-547 https://doi.org/10.1175/1520-0442(1988)001<0523:tiopeo>2.0.co;2.

Dorigo, W., De Jeu, R., Chung, D., Parinussa, R., Liu, Y., Wagner, W., Fernández-Prieto, D., (2012). "Evaluating global trends (1988-2010) in harmonized multi-satellite surface soil moisture". *Geophys. Res. Lett*. 39, L18405. https://doi.org/10.1029/2012GL052988

Dorigo, W., Wagner, W., Albergel, C., Albrecht, F., Balsamo, G., Brocca, L., Chung, D., Ertl, M., Forkel, M., Gruber, A., Haas, E., Hamer, P.D., Hirschi, M., Ikonen, J., de Jeu, R., Kidd, R., Lahoz, W., Liu, Y.Y., Miralles, D., Mistelbauer, T., Nicolai-Shaw, N., Parinussa, R., Pratola, C., Reimer, C., van der Schalie, R., Seneviratne, S.I., Smolander, T., Lecomte, P., (2017). "ESA CCI Soil Moisture for improved Earth system understanding: State-of-the art and future directions". *Remote Sens. Environ.* 185-215. https://doi.org/10.1016/j.rse.2017.07.001

Dorigo, W.A., Gruber, A., De Jeu, R.A.M., Wagner, W., Stacke, T., Loew, A., Albergel, C., Brocca, L., Chung, D., Parinussa, R.M., Kidd, R., (2015). "Evaluation of the ESA CCI soil moisture product using ground-based observations". *Remote Sens. Environ*. 162, 380-395 https://doi.org/10.1016/j.rse.2014.07.023

ESA CCI ECV SM Product User Guide - Retrivied from: https://esa-soilmoisture-cci.org/sites/default/files/documents/public/CCI%20SM%20v05.2%20documentation/ESA_CCI_SM_RD_D4.2_v1_Product_Users_Guide_v05.2.pdf. Accessed on 2 February 2020

EFFIS – Retrivied from: https://effis.jrc.ec.europa.eu/reports-and-publications/annual-fire-reports. Accessed on 1 July 2020

EMDAT - Retrivied from: https://www.emdat.be/database. Accessed on 16 June 2020.

Falkowski, P., Scholes, R.J., Boyle, E., Canadell, J., Canfield, D., Elser, J., Gruber, N., Hibbard, K., Hogberg, P., Linder, S., Mackenzie, F.T., Moore, B., Pedersen, T., Rosental, Y., Seitzinger, S., Smetacek, V., Steffen, W., (2000). "The global carbon cycle: A test of our knowledge of earth as a system". *Science* 290, 291-296. https://doi.org/10.1126/science.290.5490.291

Farooq, M., Wahid, A., Kobayashi, N., Fujita, D., Basra, S.M.A., (2009). "Plant drought stress: Effects, mechanisms and management" *Sustainable Agriculture*. 153-188. https://doi.org/10.1007/978-90-481-2666-8_12

Flach, M., Sippel, S., Gans, F., Bastos, A., Brenning, A., Reichstein, M., Mahecha, M.D., (2018). "Contrasting biosphere responses to hydrometeorological extremes: Revisiting the 2010 western Russian heatwave". *Biogeosciences*. 15, 6067-6085. https://doi.org/10.5194/bg-15-6067-2018

Flannigan, M.D., Amiro, B.D., Logan, K.A., Stocks, B.J., Wotton, B.M., (2006). "Forest fires and climate change in the 21ST century" *Mitigation and Adaptation Strategies for Global Change*. 11, 847-859. https://doi.org/10.1007/s11027-005-9020-7

Frank, Dorothea, Reichstein, M., Bahn, M., Thonicke, K., Frank, David, Mahecha, M.D., Smith, P., van der Velde, M., Vicca, S., Babst, F., Beer, C., Buchmann, N., Canadell, J.G., Ciais, P., Cramer, W., Ibrom, A., Miglietta, F., Poulter, B., Rammig, A., Seneviratne, S.I., Walz, A., Wattenbach, M., Zavala, M.A., Zscheischler, J., (2015). "Effects of climate extremes on the terrestrial carbon cycle: Concepts, processes and potential future impacts". *Glob. Chang. Biol.* 21, 2861-2880. https://doi.org/10.1111/gcb.12916

Friedl, M.A., Sulla-Menashe, D., Tan, B., Schneider, A., Ramankutty, N., Sibley, A., Huang, X., (2010). "MODIS Collection 5 global land cover: Algorithm refinements and characterization of new datasets". *Remote Sens. Environ* . 114(1), 168-182. https://doi.org/10.1016/j.rse.2009.08.016

Friedlingstein, P., Jones, M.W., O'Sullivan, M., Andrew, R.M., Hauck, J., Peters, G.P., Peters, W., Pongratz, J., Sitch, S., Le Quéré, C., DBakker, O.C.E., Canadell1, J.G., Ciais1, P., Jackson, R.B.,

Anthoni1, P., Barbero, L., Bastos, A., Bastrikov, V., Becker, M., Bopp, L., Buitenhuis, E., Chandra, N., Chevallier, F., Chini, L.P., Currie, K.I., Feely, R.A., Gehlen, M., Gilfillan, D., Gkritzalis, T., Goll, D.S., Gruber, N., Gutekunst, S., Harris, I., Haverd, V., Houghton, R.A., Hurtt, G., Ilyina, T., Jain, A.K., Joetzjer, E., Kaplan, J.O., Kato, E., Goldewijk, K.K., Korsbakken, J.I., Landschützer, P., Lauvset, S.K., Lefèvre, N., Lenton, A., Lienert, S., Lombardozzi, D., Marland, G., McGuire, P.C., Melton, J.R., Metzl, N., Munro, D.R., Nabel, J.E.M.S., Nakaoka, S.I., Neill, C., Omar, A.M., Ono, T., Peregon, A., Pierrot, D., Poulter, B., Rehder, G., Resplandy, L., Robertson, E., Rödenbeck, C., Séférian, R., Schwinger, J., Smith, N., Tans, P.P., Tian, H., Tilbrook, B., Tubiello, F.N., Van Der Werf, G.R., Wiltshire, A.J., Zaehle, S., (2019). "Global carbon budget 2019". *Earth Syst. Sci. Data*. 11, 1783-1838. https://doi.org/10.5194/essd-11-1783-2019

García-Herrera, R., Paredes, D., Trigo, R.M., Trigo, I.F., Hernández, E., Barriopedro, D., Mendes, M.A., (2007). "The outstanding 2004/05 drought in the Iberian Peninsula: Associated atmospheric circulation". *J. Hydrometeorol*. 8, 483-498. https://doi.org/10.1175/JHM578.1

Gouveia, C., DaCamara, C.C., Trigo, R.M., (2010). "Post-fire vegetation recovery in Portugal based on spot/vegetation data". *Nat. Hazards Earth Syst. Sci.* 10, 673-684. https://doi.org/10.5194/nhess-10-673-2010

Gouveia, C., Trigo, R.M., DaCamara, C.C., (2009). "Drought and vegetation stress monitoring in Portugal using satellite data". *Nat. Hazards Earth Syst. Sci.* 9, 185-195. https://doi.org/10.5194/nhess-9-185-2009

Gouveia, C.M., Bastos, A., Trigo, R.M., Dacamara, C.C., (2012). "Drought impacts on vegetation in the pre- and post-fire events over Iberian Peninsula". *Nat. Hazards Earth Syst. Sci.* 12, 3123-3137. https://doi.org/10.5194/nhess-12-3123-2012

Gouveia, C.M., Bistinas, I., Liberato, M.L.R., Bastos, A., Koutsias, N., Trigo, R., (2016). "The outstanding synergy between drought, heatwaves and fuel on the 2007 Southern Greece exceptional fire season". *Agric. For. Meteorol.* 218-219, 135-145. https://doi.org/10.1016/j.agrformet.2015.11.023

Grillakis, M.G., (2019). "Increase in severe and extreme soil moisture droughts for Europe under climate change". *Sci. Total Environ.* 660, 1245-1255. https://doi.org/10.1016/j.scitotenv.2019.01.001

Helbig, M., Chasmer, L.E., Desai, A.R., Kljun, N., Quinton, W.L., Sonnentag, O., (2017). "Direct and indirect climate change effects on carbon dioxide fluxes in a thawing boreal forest–wetland landscape". *Glob. Chang. Biol*. 23, 3231-3248. https://doi.org/10.1111/gcb.13638

Hirschi, M., Seneviratne, S.I., Alexandrov, V., Boberg, F., Boroneant, C., Christensen, O.B., Formayer, H., Orlowsky, B., Stepanek, P., (2011). "Observational evidence for soil-moisture impact on hot extremes in southeastern Europe". *Nat. Geosci*. 4, 17-21. https://doi.org/10.1038/ngeo1032

ICNF (2017). "10.º RELATÓRIO PROVISÓRIO DE INCÊNDIOS FLORESTAIS – 2017". Retrieved from: http://www2.icnf.pt/portal/florestas/dfci/Resource/doc/rel/2017/10-rel-prov-1jan-31out-2017.pdf. Accessed on 15 October 2020

IPCC. (2018). "Global Warming of 1.5 °C". Retrieved from: https://www.ipcc.ch/site/assets/uploads/sites/2/2019/06/SR15_Full_Report_High_Res.pdf. Accessed on 3 March 2020

Kaplan, J.O., Krumhardt, K.M., Zimmermann, N.E., (2012). "The effects of land use and climate change on the carbon cycle of Europe over the past 500 years". *Glob. Chang. Biol.* 18, 902-914. https://doi.org/10.1111/j.1365-2486.2011.02580.x

Koutsias, N., Arianoutsou, M., Kallimanis, A.S., Mallinis, G., Halley, J.M., Dimopoulos, P., (2012). "Where did the fires burn in Peloponnisos, Greece the summer of 2007? Evidence for a synergy of fuel and weather". *Agric. For. Meteorol*. 156, 41-53.

https://doi.org/10.1016/j.agrformet.2011.12.006

Liu, Y.Y., Parinussa, R.M., Dorigo, W.A., De Jeu, R.A.M., Wagner, W., M. Van Dijk, A.I.J., McCabe, M.F., Evans, J.P., (2011). "Developing an improved soil moisture dataset by blending passive and active microwave satellite-based retrievals". *Hydrol. Earth Syst. Sci*. 15, 425-436. https://doi.org/10.5194/hess-15-425-2011

Lizundia-Loiola, J., Otón, G., Ramo, R., Chuvieco, E., (2020). "A spatio-temporal active-fire clustering approach for global burned area mapping at 250 m from MODIS data". *Remote Sens. Environ*. 236, 111493. https://doi.org/10.1016/j.rse.2019.111493

Mahowald, N.M., Ward, D.S., Doney, S.C., Hess, P.G., Randerson, J.T., (2017). "Are the impacts of land use on warming underestimated in climate policy?" *Environ. Res. Lett*. 12, 094016. https://doi.org/10.1088/1748-9326/aa836d

Martínez-Fernández, J., González-Zamora, A., Sánchez, N., Gumuzzio, A., Herrero-Jiménez, C.M., (2016). "Satellite soil moisture for agricultural drought monitoring: Assessment of the SMOS derived Soil Water Deficit Index". *Remote Sens. Environ*. 177, 277-286. https://doi.org/10.1016/j.rse.2016.02.064

Melillo, J.M., McGuire, A.D., Kicklighter, D.W., Moore, B., Vorosmarty, C.J., Schloss, A.L., (1993). "Global climate change and terrestrial net primary production". *Nature.* 363, 234–240. https://doi.org/10.1038/363234a0

Monteith, J.L., (1972). "Solar Radiation and Productivity in Tropical Ecosystems". *J. Appl. Ecol*. 9(3), 747-766. https://doi.org/10.2307/2401901

Padilla, M., Wheeler, J., Tansey K., (2018), "ESA CCI ECV Fire Disturbance: D4.1.1. Product Validation Report, version 2.1. Tech. Rep. Retrivied from: https://www.esa-fire-cci.org/sites/default/files/Fire_cci_D4.1.1_PVR_v2.1_0.pdf. Accessed on 26 September 2020.

Pereira, M.G., Trigo, R.M., Da Camara, C.C., Pereira, J.M.C., Leite, S.M., (2005). "Synoptic patterns associated with large summer forest fires in Portugal". *Agric. For. Meteorol*. 129, 11-25. https://doi.org/10.1016/j.agrformet.2004.12.007

Powers, R.P., Jetz, W., (2019). "Global habitat loss and extinction risk of terrestrial vertebrates under future land-use-change scenarios". *Nat. Clim. Chang*. 9, 323-329. https://doi.org/10.1038/s41558-019-0406-z

Rebetez, M., Dupont, O., Giroud, M., (2009). "An analysis of the July 2006 heatwave extent in Europe compared to the record year of 2003". *Theor. Appl. Climatol*. 95, 1-7. https://doi.org/10.1007/s00704-007-0370-9

Reichstein, M., Bahn, M., Ciais, P., Frank, D., Mahecha, M.D., Seneviratne, S.I., Zscheischler, J., Beer, C., Buchmann, N., Frank, D.C., Papale, D., Rammig, A., Smith, P., Thonicke, K., Van Der Velde, M., Vicca, S., Walz, A., Wattenbach, M., (2013). "Climate extremes and the carbon cycle Climate extremes and the biosphere". *Nature* 500, 287-295. https://doi:10.1038/nature12350

Rubio, M.A., López, G., Tovar, J., Pozo, D., Batlles, F.J., (2005). "The use of satellite measurements to estimate photosynthetically active radiation". *Phys. Chem. Earth*. 30, 159-164. https://doi.org/10.1016/j.pce.2004.08.029

Ruffault, J., Curt, T., Martin-StPaul, N.K., Moron, V., Trigo, R.M., (2018). "Extreme wildfire events are linked to global-change-type droughts in the northern Mediterranean". *Nat. Hazards Earth Syst. Sci.*, 18, 847-856. https://doi.org/10.5194/nhess-18-847-2018

Ruffault, J., Moron, V., Trigo, R.M., Curt, T., (2017). "Daily synoptic conditions associated with large fire occurrence in Mediterranean France: evidence for a wind-driven fire regime". *Int. J. Climatol*. 37, 524-533. https://doi.org/10.1002/joc.4680

Running, S.W., Nemani, R.R., Heinsch, F.A., Zhao, M., Reeves, M., Hashimoto, H., (2004). "A continuous satellite-derived measure of global terrestrial primary production". *Bioscience*. 54,

547-560. https://doi.org/10.1641/0006-3568(2004)054[0547:ACSMOG]2.0.CO;2

Running, S.W., Thornton, P.E., Nemani, R., Glassy, J.M., (2000). "Global Terrestrial Gross and Net Primary Productivity from the Earth Observing System, in: Methods in Ecosystem Science". *Springer* New York, pp. 44–57. https://doi.org/10.1007/978-1-4612-1224-9_4

Russo, A., Gouveia, C.M., Páscoa, P., DaCamara, C.C., Sousa, P.M., Trigo, R.M., (2017). "Assessing the role of drought events on wildfires in the Iberian Peninsula". *Agric. For. Meteorol*. 237-238, 50-59. https://doi.org/10.1016/j.agrformet.2017.01.021

Sala, A., Woodruff, D.R., Meinzer, F.C., (2012). "Carbon dynamics in trees: Feast or famine?" *Tree Physiol*. 32, 764-775. https://doi.org/10.1093/treephys/tpr143

Sánchez-Benítez, A., García-Herrera, R., Barriopedro, D., Sousa, P.M., Trigo, R.M., (2018). "June 2017: The Earliest European Summer Mega-heatwave of Reanalysis Period". *Geophys. Res. Lett*. 45, 1955-1962. https://doi.org/10.1002/2018GL077253

Sippel, S., Reichstein, M., Ma, X., Mahecha, M.D., Lange, H., Flach, M., Frank, D., (2018). "Drought, Heat, and the Carbon Cycle: a Review". *Curr. Clim. Chang. Reports*. 4, 266-286. https://doi.org/10.1007/s40641-018-0103-4

Smith, M.D., (2011). "An ecological perspective on extreme climatic events: A synthetic definition and framework to guide future research". *J. Ecol*. 99, 656-663. https://doi.org/10.1111/j.1365-2745.2011.01798.x

Spinoni, J., Vogt, J. V., Naumann, G., Barbosa, P., Dosio, A., (2018). "Will drought events become more frequent and severe in Europe?" *Int. J. Climatol*. 38, 1718-1736. https://doi.org/10.1002/joc.5291

Tolika, K., Maheras, P., Tegoulias, I., (2009). "Extreme temperatures in Greece during 2007: Could this be a "return to the future"?" *Geophys. Res. Lett*. 36, L10813. https://doi.org/10.1029/2009GL038538

Trigo, R.M., Pereira, J.M.C., Pereira, M.G., Mota, B., Calado, T.J., Dacamara, C.C., Santo, F.E., (2006). "Atmospheric conditions associated with the exceptional fire season of 2003 in Portugal". *Int. J. Climatol*. 26, 1741-1757. https://doi.org/10.1002/joc.1333

Turco, M., Von Hardenberg, J., AghaKouchak, A., Llasat, M.C., Provenzale, A., Trigo, R.M., (2017). "On the key role of droughts in the dynamics of summer fires in Mediterranean Europe". *Sci. Rep*. 7:81 https://doi.org/10.1038/s41598-017-00116-9

Turner, D.P., Ritts, W.D., Cohen, W.B., Gower, S.T., Running, S.W., Zhao, M., Costa, M.H., Kirschbaum, A.A., Ham, J.M., Saleska, S.R., Ahl, D.E., (2006). "Evaluation of MODIS NPP and GPP products across multiple biomes". *Remote Sens. Environ*. 102, 282-292. https://doi.org/10.1016/j.rse.2006.02.017

Turner, D.P., Ritts, W.D., Cohen, W.B., Maeirsperger, T.K., Gower, S.T., Kirschbaum, A.A., Running, S.W., Zhao, M., Wofsy, S.C., Dunn, A.L., Law, B.E., Campbell, J.L., Oechel, W.C., Kwon, H.J., Meyers, T.P., Small, E.E., Kurc, S.A., Gamon, J.A., (2005). "Site-level evaluation of satellite-based global terrestrial gross primary production and net primary production monitoring". *Glob. Chang. Biol*. 11, 666-684. https://doi.org/10.1111/j.1365-2486.2005.00936.x

Ueyama, M., Iwata, H., Harazono, Y., Euskirchen, E.S., Oechel, W.C., Zona, D., (2013). "Growing season and spatial variations of carbon fluxes of Arctic and boreal ecosystems in Alaska (USA)". *Ecol. Appl*. 23(8), 1798-1816. https://doi.org/10.1890/11-0875.1

Ulaby, F.T., Moore, R.K., Fung, A.K., (1982). Microwave remote sensing: active and passive. Volume II. Radar remote sensing and surface scattering and emission theory. Microw. Remote Sens. Act. Passiv. Vol. II. Radar Remote Sens. Surf. Scatt. Emiss. theory.

Waring, R.H., Running, S.S., (2007). "Forest Ecosystems", Forest Ecosystems. https://doi.org/10.1016/B978-0-12-370605-8.X5001-4

White, J.D., Running, S.W., (1994). "Testing scale dependent assumptions in regional ecosystem simulations". *J. Veg. Sci*. 5, 687-702 https://doi.org/10.2307/3235883

Zscheischler, J., Westra, S., Van Den Hurk, B.J.J.M., Seneviratne, S.I., Ward, P.J., Pitman, A., Aghakouchak, A., Bresch, D.N., Leonard, M., Wahl, T., Zhang, X., (2018). "Future climate risk from compound events". *Nat. Clim. Chang*. 8, 469-477. https://doi.org/10.1038/s41558-018-0156-3

Appendix

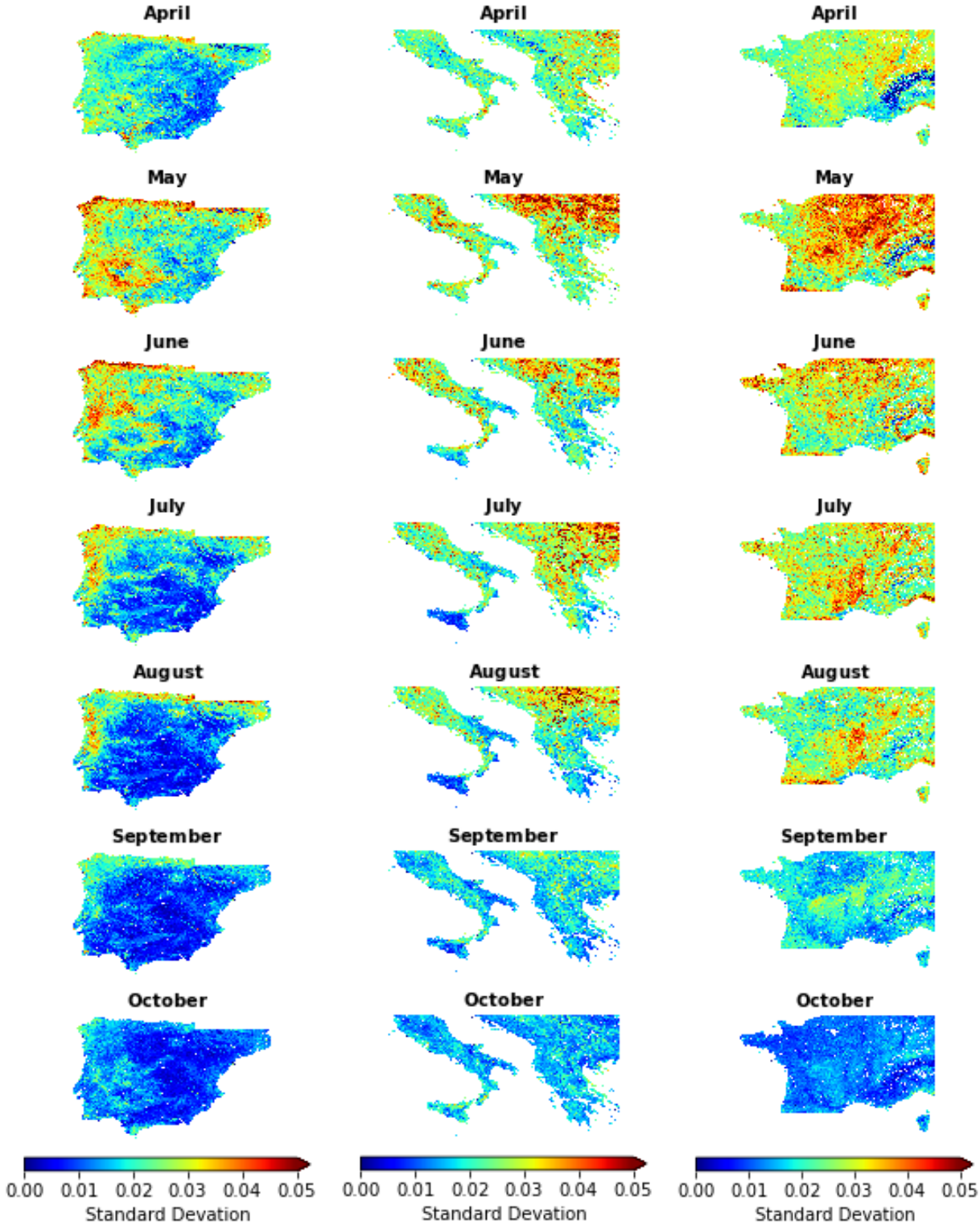

Figure A.1 – Temporal GPP monthly standard deviation for the three study regions, between April and October.

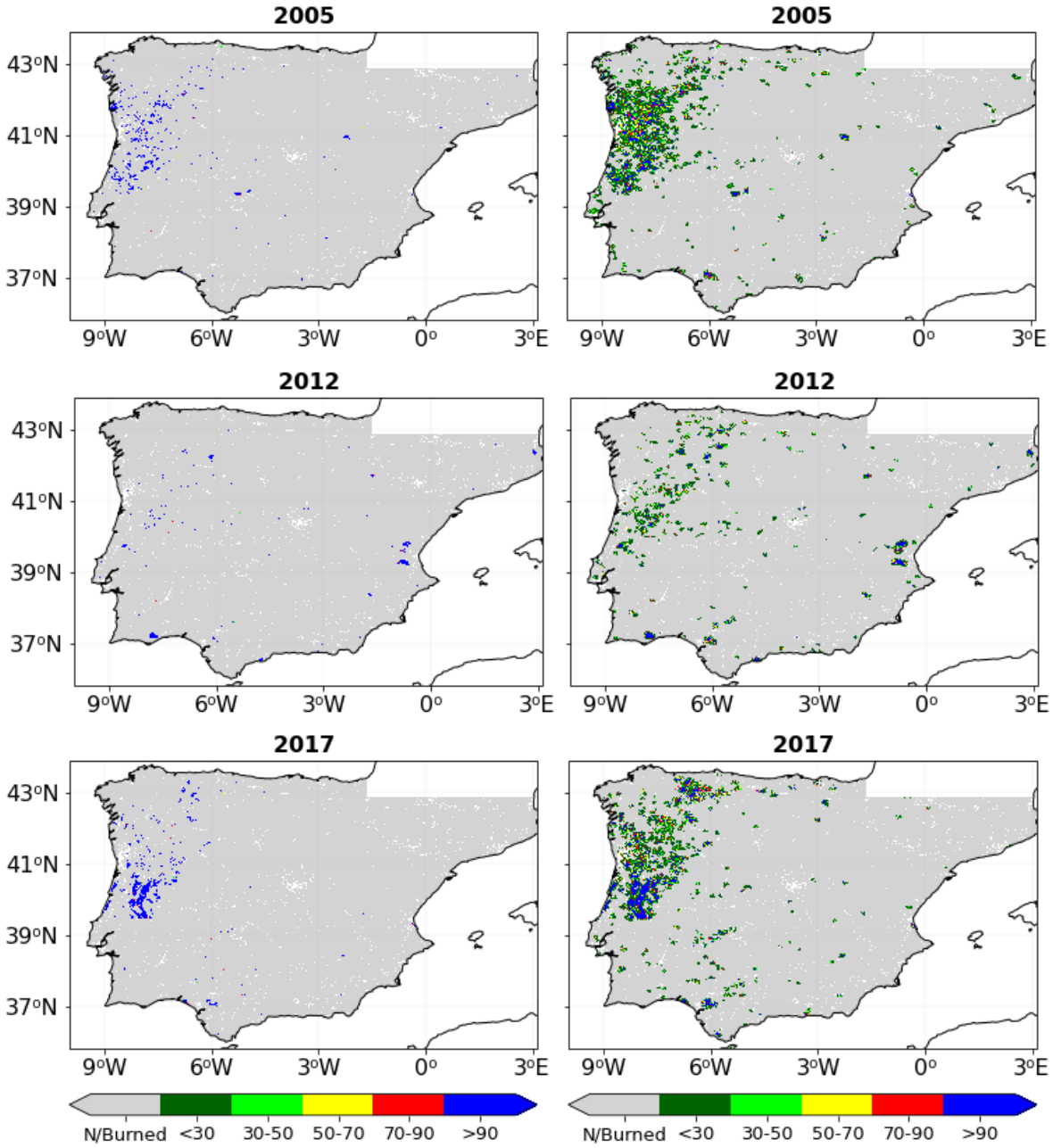

Figure A.2 - Level of confidence of detected burned pixels (left panel) and of all the detected pixels incorporated on CL dataset (right panel) for IB in 2005 (top panels), 2012 (central panels) and 2017 (bottom panels).

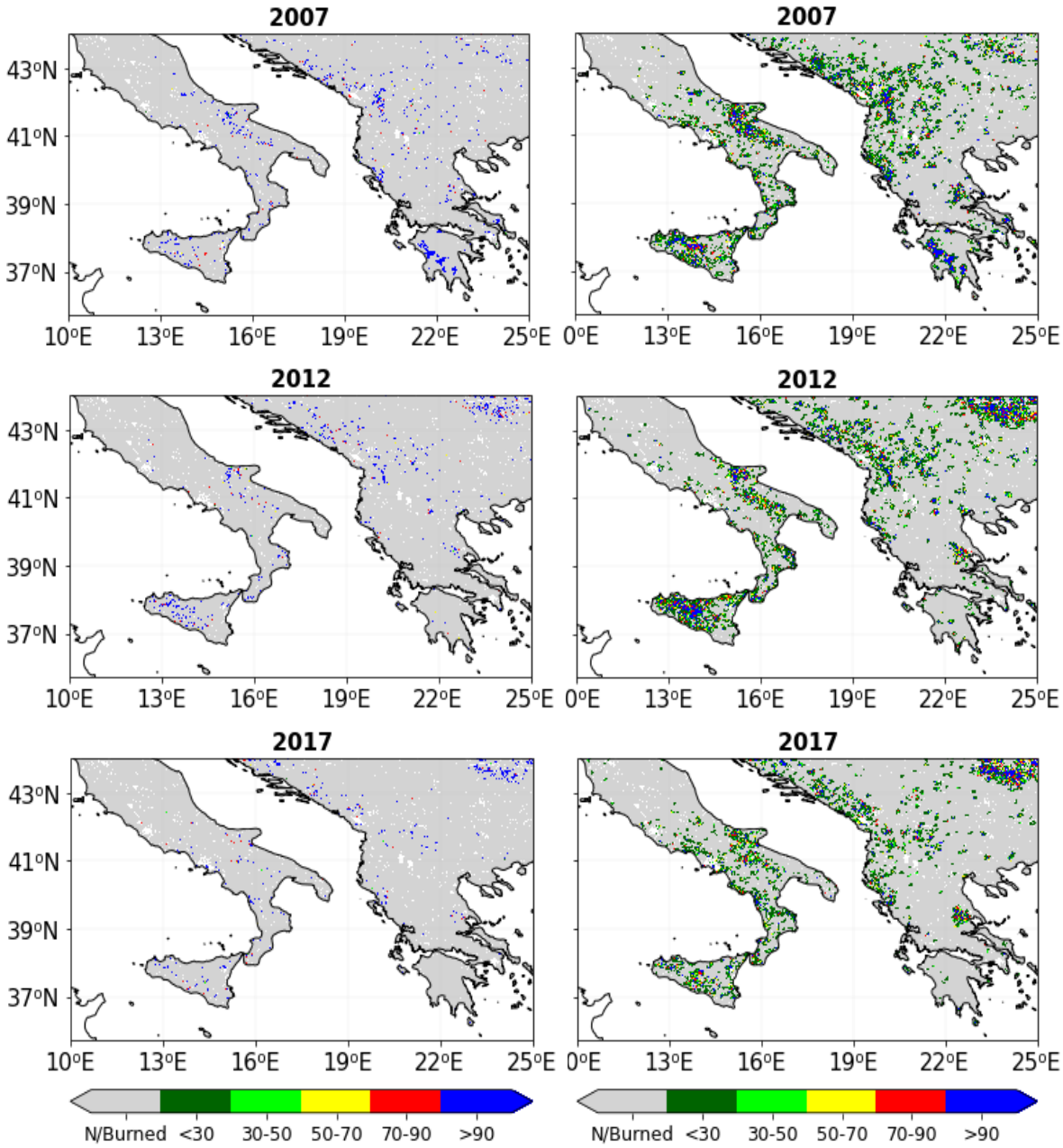

Figure A.3 - As in Figure A.2 but respecting to IG region in 2007 (top panels), 2012 (middle panels) and 2017 (bottom panels).

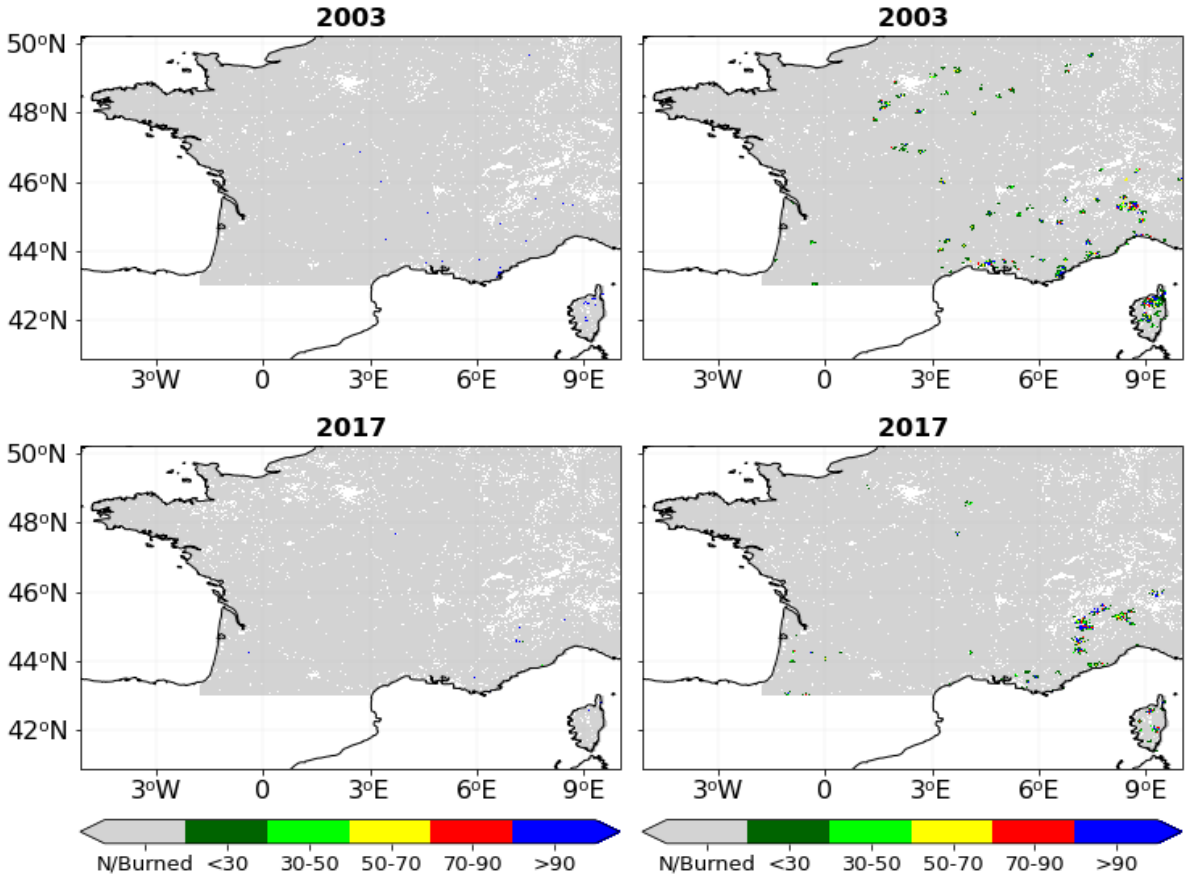

Figure A.4 - As in Figure A.2 but respecting to FR region in 2003 (top panels) and 2017 (bottom panels).